

Completely positive trace-preserving maps for higher-order unraveling of Lindblad master equations

Nattaphong Wonglakhon¹, Howard M. Wiseman¹, and Areeya Chantasri^{1,2}

¹*Centre for Quantum Computation and Communication Technology (Australian Research Council),
Centre for Quantum Dynamics, Griffith University,
Yuggera Country, Brisbane, Queensland 4111, Australia*

²*Optical and Quantum Physics Laboratory, Department of Physics,
Faculty of Science, Mahidol University, Bangkok 10400, Thailand*

(Dated: August 27, 2024)

Theoretical tools used in processing continuous measurement records from real experiments to obtain quantum trajectories can easily lead to numerical errors due to a non-infinitesimal time resolution. In this work, we propose a systematic assessment of the accuracy of a map. We perform error analyses for diffusive quantum trajectories, based on single-time-step Kraus operators proposed in the literature, and find the orders in time increment, Δt , to which such operators satisfy the conditions for valid average quantum evolution (completely positive, convex-linear, and trace-preserving), and the orders to which they match the Lindblad solutions. Given these error analyses, we propose a Kraus operator that satisfies the valid average quantum evolution conditions and agrees with the Lindblad master equation, to second order in Δt , thus surpassing all other existing approaches. In order to test how well our proposed operator reproduces exact quantum trajectories, we analyze two examples of qubit measurement, where exact maps can be derived: a qubit subjected to a dispersive (z -basis) measurement and a fluorescence (dissipative) measurement. We show analytically that our proposed operator gives the smallest average trace distance to the exact quantum trajectories, compared to existing approaches.

I. INTRODUCTION

Open quantum system dynamics describes state evolutions of quantum systems of interest that interact with their environment (bath) [1–3]. The resulting system dynamics not only depends on the interactions with the bath, but also on whether the bath’s actual states are unknown or known to observers [4, 5], leading to decoherence effects or measurement backactions on the system’s state, respectively. Under the strong Markov assumption [6], if the bath’s state is unknown, the system’s dynamics, after tracing out the bath degree of freedom, exhibits the decoherence described by the Lindblad master equation [7, 8]. However, if the bath’s state is revealed, via measurement, the system’s state can be estimated *conditioned* on measurement outcomes. For continuous quantum measurement, a realization of the measurement record is stochastic by nature, leading to a stochastic conditioned state dynamic referred to as a *quantum trajectory* or *quantum state filtering* [5, 9, 10]. The quantum trajectory can also be considered as a result of *unraveling* the Lindblad master equation, because, by averaging the conditioned dynamics over all possible measurement records, their average coincides with the solution of the master equation, see Fig. 1(a).

To unravel the Lindblad master equation using continuous quantum measurement, many theoretical formulations have been proposed and even implemented in real experiments. The most common form of unraveling is via stochastic Schrödinger equations (SSEs) and stochastic master equations (SMEs) [11, 12], which can be derived from quantum (filtering) stochastic calculus [13–15], from system-bath interactions in quantum

optics [4, 16–19], or from phenomenological Bayesian-type update equations [20, 21]. The SSEs and SMEs have been the basic formalisms used in describing stochastic quantum evolutions [18, 22–24], for qubits and other quantum systems; see Refs. [25–29] for recent work. However, such SMEs are typically written with the assumption that the noisy measurement records from weak (diffusive) measurements can be written as a sum of signal parts and Gaussian white noises. This is only strictly valid for the continuous time limit, i.e., when the time increment is assumed infinitesimal (dt). Unfortunately, measurement records from real experiments are obtained with finite time resolution, denoted by Δt . Therefore, directly using the SMEs to process the finite-time discretized experimental data likely results in numerical errors. For example, directly integrating an SME for quantum states when the time step is not small enough can result in quantum states being non positive semi-definite or even not normalized [30–33].

There have been proposed workarounds to reduce such numerical errors by, instead of integrating SMEs, computing quantum state evolutions via Δt -discretized maps, using some approximated measurement operators or maps. In the early work to verify quantum trajectories from homodyne signals in superconducting circuits [34–38], the quantum states were computed with maps constructed from Bayesian probabilities, which could give exact quantum evolutions, but only for Hermitian measured observables. For a more general treatment, a positivity preserving formulation [30, 32] has also been used in processing superconducting qubit’s heterodyne fluorescence measurement [39–41], or even combined with a strongly convergent stochastic integration method such

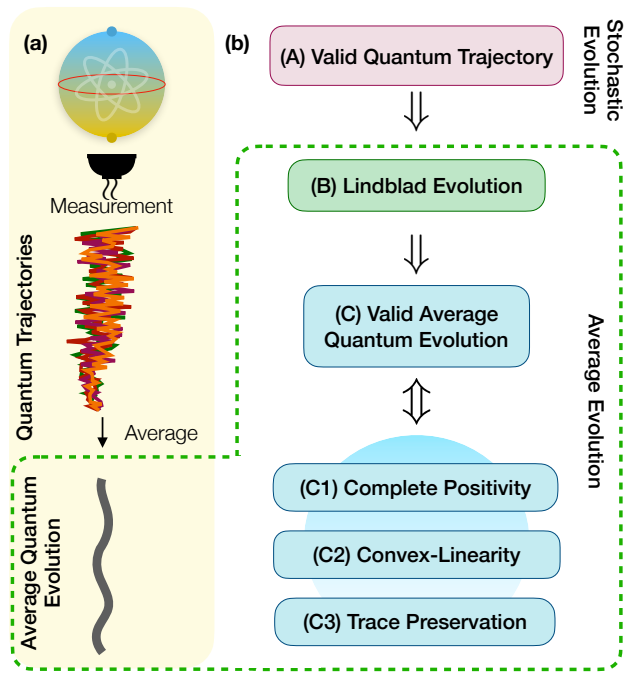


FIG. 1. Diagrams show evolutions of open quantum systems and their hierarchy criteria. (a) Schematic diagrams showing a qubit measured continuously in time, resulting in quantum trajectories. (b) Hierarchy conditions (A), (B), and (C1)-(C3) and their implications are indicated by double-line arrows. If a map satisfies (A) should automatically satisfy (B) and (C1)-(C3), but not in a reverse direction (see text for more detail). Components inside the green dashed box are applied to average quantum evolutions.

as the Euler-Milstein [33, 42]. However, as we show in this work, those maps reproduce the Lindblad evolution, and generate valid average quantum evolution, with an accuracy only to first order in Δt . Even in a recently proposal by Guevara and Wiseman [43], in which the map generates valid average quantum evolution to second order in Δt , it does not reproduce the Lindblad evolution to the same accuracy. This means that quantum trajectories generated with all the above approaches only average to the Lindblad solution to first order in Δt .

In this work, we present a systematic way to analyze what should be a good map in quantum trajectory theory. The diagram in Fig. 1(b) shows a hierarchy of conditions. The strongest one is (A) *valid quantum trajectory*. This means that each trajectory generated with a finite Δt agrees, to some order in Δt (suitably defined), to the corresponding exact trajectory which would be generated with $\Delta t \rightarrow dt$, where dt is an infinitesimal time. If this is satisfied, then the average evolution will satisfy (B) *Lindblad evolution*, to the same order in Δt . In turn, satisfying the Lindblad evolution means the trajectories on average also satisfy (C) *valid average quantum evolution*, to the same order in Δt . This last can be broken into three conditions that must be satisfied: (C1) *Com-*

plete positivity, (C2) *Convex-linearity*, and (C3) *Trace preservation*. These ideas will be made more precise in Section II.

None of the one-way implications in Fig. 1(b) work in the reverse direction. For example, the Guevara-Wiseman map [43], satisfies (C) to second order in Δt , but satisfies (B) only to first order. This was stated explicitly in Ref. [43], but other higher-order approaches have not been analyzed according to this hierarchy. In this paper, we analyze these existing map systematically and show their Δt order of error in the hierarchy (A)-(C), also using the breakdown (C1)-(C3). We show that all existing approaches satisfy (B) only at the first order in Δt . This brings us to propose a higher-order measurement map, which we call the W-map, constructed from a unitary system-bath interaction expanded to fourth order in the bath operator. This W-map satisfies the conditions (B) and (C1)-(C3), all to the second order in Δt .

On the level of individual trajectory, we can also check whether condition (A) is satisfied to higher order for some specific instances, where *exact* (or nearly exact) finite-time solutions for quantum trajectories can be derived analytically. This is done for two qubit examples: the qubit continuous z -measurement, and the fluorescence homodyne measurement. We calculate how closely each of the Δt -maps is to the corresponding map from the exact quantum trajectories, and average over all an ensemble of records. We show that our proposed W-map gives the best accuracy among all existing methods, although there is no difference in scaling with Δt for any of the measurement operators we consider. Achieving (A) to higher order is thus still an open problem for higher order quantum trajectory theory.

The paper is organized as the follows. In Section II, we summarize theories for open quantum systems, describing conditioned (measurement) evolution, unconditioned (Lindblad) evolution, and valid average quantum evolution, along with introducing properties (A), (B), and (C1)-(C3). Here measurement operators and their properties are defined. In Section III, we investigate measurement operators of existing approaches in the literature: the standard Itô map, the Euler-Milstein approach [33], and the so-called completely positive map [43]. In Section IV, we derive our W-map, from a system coupled to a bosonic (harmonic-oscillator) bath, and show that it satisfies properties (B) and (C) to second order in Δt . We then consider the two qubit examples of continuous z -measurement and homodyne fluorescence measurement, in Section VI, showing the deviation of individual quantum trajectories from their exact counterparts for all the approaches. Section VII concludes.

II. OPEN QUANTUM SYSTEM AND MEASUREMENT OPERATION

Let us consider the time evolution of a quantum system interacting with its environment (or bath). The system

and the bath together, called a combined system, can be treated as a closed quantum system, where its evolution can be described by a unitary evolution with a specific Hamiltonian. Pure quantum states of the combined system live in a tensor product of individual Hilbert spaces, $\mathcal{H}_s \otimes \mathcal{H}_e$, where \mathcal{H}_s and \mathcal{H}_e are the Hilbert spaces of the system of interest and its bath, respectively. For applications in continuous measurement under the strong Markov assumption, we assume that the system interacts with its bath for a short interval between time t and $t + \Delta t$ and that the combined system at the start of any interval is in a product state $\varrho(t) = \rho(t) \otimes |e_0\rangle\langle e_0|$, where $|e_0\rangle\langle e_0|$ is the initial bath's state. In our work, we do not assume the time interval Δt to be infinitesimally small in order to investigate effects from its being finite. The unitary evolution of the combined system is described by

$$\varrho(t + \Delta t) = \hat{U}_{t+\Delta t, t} (\rho(t) \otimes |e_0\rangle\langle e_0|) \hat{U}_{t+\Delta t, t}^\dagger, \quad (1)$$

where $\hat{U}_{t+\Delta t, t}$ is the unitary operator for the combined system. After the evolution in Eq. (1), the system may become entangled with the bath.

A. Conditioned state evolution on measurement readouts

Let us consider a scenario where there is an observation, i.e., the bath's state is measured by an observer with some detection scheme. The system's state evolution should therefore reflect the information gained from the measurement readouts. To describe the bath's detection, we consider collapse of the bath's state to one of the eigenstates of the bath's measured observable. Let us define one of the eigenstates by $|e_r\rangle \in \{|e_k\rangle\}$, which also corresponds to a particular observed readout (' r ' stands for 'readout'). The conditioned system's state, after tracing out the bath's degrees of freedom from the combined system's state, $\varrho(t + \Delta t)$, in Eq. (1), becomes

$$\begin{aligned} \rho_r(t + \Delta t) &\propto \text{Tr}_e[|e_r\rangle\langle e_r| \varrho(t + \Delta t)] \\ &= \hat{K}(r) \rho(t) \hat{K}^\dagger(r) \equiv \tilde{\mathcal{J}}[\hat{K}(r)] \rho(t), \end{aligned} \quad (2)$$

where a superoperator $\tilde{\mathcal{J}}[\hat{A}] \bullet \equiv \hat{A} \bullet \hat{A}^\dagger$ represents a linear map with an operator \hat{A} . Noting that the equations on the right side are not normalized. In the second line, we have defined a measurement operator

$$\hat{K}(r) = \langle e_r | \hat{U}_{t+\Delta t, t} | e_0 \rangle, \quad (3)$$

commonly known as a Kraus operator. We note that Eq. (2), even though not normalized, has a linear property in the quantum state and can be used in generating *linear* quantum trajectories [5, 44, 45]. These play an important role in the quantum state retrodiction [46], the two-state formalism [47] and the quantum state smoothing [43, 48, 49], as will be explained in Sec. II C.

By normalizing Eq. (2), we obtain a nonlinear superoperator,

$$\rho_r(t + \Delta t) = \frac{\hat{K}(r) \rho(t) \hat{K}^\dagger(r)}{\text{Tr}[\hat{K}(r) \rho(t) \hat{K}^\dagger(r)]} \equiv \tilde{\mathcal{J}}[\hat{K}(r)] \rho(t), \quad (4)$$

which "maps" a quantum state $\rho(t)$ at time t to a new state $\rho(t + \Delta t)$ at the later time via the Kraus operator $\hat{K}(r)$. This nonlinear map is commonly used in generating a so-called *normalized* state for the trajectories.

Properties of the $\hat{K}(r)$ operator are closely related to statistics of the measurement readout r . The denominator of Eq. (4) is to be interpreted as the probability (or probability density for the case of continuous r) of getting the readout given that the system's state before the measurement was $\rho(t)$. That is to say, the probability density function (PDF) is

$$\wp(r | \rho(t)) = \text{Tr}[\hat{K}(r) \rho(t) \hat{K}^\dagger(r)], \quad (5)$$

which can be used in computing various statistical quantities such as the mean readout and its variance,

$$\mu = \text{E}\{r\}, \quad (6a)$$

$$\sigma^2 = \text{E}\{r^2\} - \text{E}\{r\}^2, \quad (6b)$$

where we have defined the expectation value notation, which will be used throughout the paper,

$$\text{E}\{f(r)\} \equiv \int dr \wp(r | \rho(t)) f(r), \quad (7)$$

for any function of the readout r . Therefore, given Eq. (5) and its normalization condition, the Kraus operator should satisfy a *completeness relation*

$$\int dr \hat{K}^\dagger(r) \hat{K}(r) = \hat{1}, \quad (8)$$

which is the identity in the system's state space. One can also get the same condition by using Eq. (3) and show that $\int dr \langle e_0 | \hat{U}_{t+\Delta t, t}^\dagger | e_r \rangle \langle e_r | \hat{U}_{t+\Delta t, t} | e_0 \rangle = \hat{1}$, where the integral over all possible readouts of the bath gives the identity in the bath's state space, i.e., $\int dr |e_r\rangle\langle e_r| = \hat{1}_e$. This condition Eq. (8) is also called a trace-preserving condition for a map with Kraus operators.

However, the Kraus operator, $\hat{K}(r)$, in the form of Eq. (3) cannot always be derived exactly, as it is a mathematically complicated object. Therefore, one usually works with approximated versions. For describing continuous-in-time measurement, the most used approximation is the expansion to first order in the time increment. This could lead to errors in the quantum state calculation, as mentioned in the introduction, when the time increment Δt of a measurement record is not really infinitesimal. Therefore, we here introduce a valid quantum trajectory condition:

Condition (A) Valid quantum trajectory. A map satisfies this condition if it generates a quantum trajectory

that matches with $\rho_r(t)$ generated from Eq. (4), using the (exact) Kraus operator in Eq. (3).

We will consider this condition in detail later in Section V, where we introduce the two examples of a qubit system with solvable exact maps.

B. Unconditioned state evolution

Continuing from Eq. (1), if the bath's state is not observed, the reduced density matrix for the system's state can be found by taking a trace over the bath, resulting in the decoherence (non-unitary evolution) on the system's state. From Eq. (1), we can write an unconditioned system's state as

$$\rho(t + \Delta t) = \text{Tr}_e [\hat{U}_{t+\Delta t, t}(\rho(t) \otimes |e_0\rangle\langle e_0|) \hat{U}_{t+\Delta t, t}^\dagger], \quad (9)$$

where the trace $\text{Tr}_e[\dots] \equiv \sum_k \langle e_k | \dots | e_k \rangle$ is defined for the eigenbases of the bath's Hilbert space. Under the Markov assumption, one finds that the reduced system's dynamics Eq. (9) can be reformulated as [7, 8],

$$\rho(t + \Delta t) = e^{\Delta t \mathcal{L} \bullet} \rho(t), \quad (10)$$

where

$$\mathcal{L} \bullet = -i[\hat{H}, \bullet] + \sum_{j=1}^N \mathcal{D}[\hat{c}_j] \bullet, \quad (11)$$

is the Lindblad superoperator. Here, the operator \hat{H} is a Hermitian operator describing unitary dynamics of the system's state, the superoperator \mathcal{D} is defined as $\mathcal{D}[\hat{c}] \bullet = \hat{c} \bullet \hat{c}^\dagger - \frac{1}{2} \{ \hat{c}^\dagger \hat{c}, \bullet \}$ describing the non-unitary dynamics, and \hat{c}_j are the Lindblad operators describing N couplings between the system and the bath. We note that we have taken $\hbar = 1$ throughout this paper.

In the time-continuum limit, as usually assumed in most works in the literature, $\Delta t \rightarrow dt$, where dt is an infinitesimal time, Eq. (10) becomes the Lindblad master equation in differential form,

$$\partial_t \rho(t) = \mathcal{L} \rho(t). \quad (12)$$

However, in experiments [35–38], Δt cannot be infinitesimal, the exact incremental evolution Eq. (10) has to be used. If the exponential cannot be solved exactly, it can be solved by expanding to some orders in the time increment Δt . The higher the order of expansion, the higher the accuracy of the state calculation.

Let us consider the case with a single Lindblad operator \hat{c} and no unitary dynamics, $\hat{H} = 0$, in order to focus on the dynamics of a single decoherence channel. The expansion to first order in Δt is trivial:

$$\rho(t + \Delta t) = (\hat{1} + \Delta t \mathcal{L}) \rho(t) = \rho(t) + \Delta t \mathcal{D}[\hat{c}] \rho(t). \quad (13)$$

Beyond that, it has been shown by Steinbach *et al.* [50] that the Taylor expansion of Eq. (10) to second order in Δt gives

$$\begin{aligned} \rho(t + \Delta t) &= \left(\hat{1} + \Delta t \mathcal{L} + \frac{1}{2} \Delta t^2 \mathcal{L}^2 \right) \rho(t), \\ &= \rho(t) + \Delta t \mathcal{D}[\hat{c}] \rho(t) + \frac{1}{2} \Delta t^2 \mathcal{D}^2[\hat{c}] \rho(t), \end{aligned} \quad (14)$$

where the double Lindblad operator can be expressed explicitly as

$$\begin{aligned} \mathcal{D}^2[\hat{c}] \rho(t) &= + \frac{1}{2} \hat{c}^\dagger \hat{c} \rho(t) \hat{c}^\dagger \hat{c} + \hat{c}^2 \rho(t) (\hat{c}^\dagger)^2 \\ &\quad + \frac{1}{4} [\rho(t) (\hat{c}^\dagger \hat{c})^2 + (\hat{c}^\dagger \hat{c})^2 \rho(t)] \\ &\quad - \frac{1}{2} [\hat{c} \rho(t) (\hat{c}^\dagger)^2 \hat{c} + \hat{c}^\dagger \hat{c}^2 \rho(t) \hat{c}^\dagger] \\ &\quad - \frac{1}{2} [\hat{c} \rho(t) \hat{c}^\dagger \hat{c} \hat{c}^\dagger + \hat{c} \hat{c}^\dagger \hat{c} \rho(t) \hat{c}^\dagger]. \end{aligned} \quad (15)$$

Moreover, the conditioned evolution Eq. (4) can also be considered as an unravelled trajectory of the unconditioned state (Lindblad) evolution, Eq. (9), where we can get back the dynamics (10) by integrating the conditioned state over all possible readouts with their probability weights. That is to say,

$$\begin{aligned} \rho(t + \Delta t) &= \text{E} \{ \tilde{\mathcal{J}}[\hat{K}(r)] \rho(t) \} \\ &= \int dr \wp(r | \rho(t)) \tilde{\mathcal{J}}[\hat{K}(r)] \rho(t) \\ &= \int dr \hat{K}(r) \rho(t) \hat{K}^\dagger(r) = e^{\Delta t \mathcal{L} \bullet} \rho(t), \end{aligned} \quad (16)$$

using the definition of $\text{E}\{\bullet\}$ in Eq. (7), gives the Lindblad evolution, where the superoperator \mathcal{L} is as defined in Eq. (11). This leads to defining our second condition:

Condition (B) Lindblad Evolution. A map satisfies this condition if it generates quantum trajectories that average to the Lindblad equation as in Eq. (16).

As we consider approximated Kraus operators in this work, we use the second-order expansion of the Lindblad evolution in Eq. (14) for evaluating the condition (B) for high-order accuracy Kraus operators. This is analyzed in detail in Section III and onward.

C. Valid average quantum evolution

Apart from the strong conditions (A) and (B), we here introduce weaker conditions that only require a map to generate a *valid* quantum evolution on average. That is, evolution that is completely positive (C1), convex-linear (C2) and trace preserving (C3). Before we dive into the definitions of these conditions, let us consider various approaches in the literature on how quantum trajectories are generated and averaged.

The first straightforward way is to generate normalized trajectories using the readout PDF $\wp(r | \rho(t))$, as shown in

Eq. (16), where the PDF is derived from Kraus operators (either exact or approximated ones),

$$\wp_{\mathbf{k}}(r|\rho(t)) = \text{Tr}[\hat{K}(r)\rho(t)\hat{K}^\dagger(r)], \quad (17)$$

with the subscript ‘k’ standing for ‘Kraus’. Therefore, if this PDF is used in generating trajectories, then their average quantum state evolution is given by:

$$\begin{aligned} \rho(t + \Delta t) &= \int dr \wp_{\mathbf{k}}(r|\rho(t)) \frac{\hat{K}(r)\rho(t)\hat{K}^\dagger(r)}{\text{Tr}[\hat{K}(r)\rho(t)\hat{K}^\dagger(r)]}, \\ &= \int dr \hat{K}(r)\rho(t)\hat{K}^\dagger(r), \end{aligned} \quad (18)$$

where the trace norm of the state exactly cancels the weight PDF. We call this as *Method I*. There are some interesting points to note here. If somehow an exact Kraus operator were available, but resulted in a complicate PDF function in Eq. (17), then it is usually not convenient to use the operator in numerically generating quantum trajectories. One can then approximate the Kraus operator as $\hat{K}(r) = \sqrt{\wp_{\text{ost}}}\hat{M}(r)$, with a simple ostensible probability \wp_{ost} , then compute the average evolution using the second line of Eq. (18). With this latter technique, the average can be numerically obtained from unnormalized (linear) states randomly generated with the ostensible probability, instead of the correct PDF, $\wp_{\mathbf{k}}(r|\rho(t))$. This approximate technique has been used in various stochastic simulations [43, 48, 49, 51, 52], especially in quantum state smoothing, when a large ensemble of trajectories is required.

The second way is to use a simple *guessed* readout PDF, $\wp_{\mathbf{g}}(r|\rho(t))$, where ‘g’ stands for ‘guess’ to compute the average quantum evolution. For instance in quantum optics [5], the distribution of a homodyne detection readout is often approximated as Gaussian. The average evolution is thus given by:

$$\rho(t + \Delta t) = \int dr \wp_{\mathbf{g}}(r|\rho(t)) \frac{\hat{K}(r)\rho(t)\hat{K}^\dagger(r)}{\text{Tr}[\hat{K}(r)\rho(t)\hat{K}^\dagger(r)]}, \quad (19)$$

and this method is called *Method II*. This method, although not quite as accurate as Method I, has advantage in numerical simulation of quantum trajectories, because a random generator with Gaussian distribution (normal distribution) is native in most programming languages.

Another common approach to compute the average quantum evolution is via an SME. By naively generating states in time steps of size Δt , this yields

$$\rho(t + \Delta t) = \rho(t) + \Delta t \mathcal{D}[\hat{c}]\rho(t) + \Delta W \mathcal{H}[\hat{c}]\rho(t), \quad (20)$$

where $\mathcal{H}[\hat{c}]\bullet \equiv \hat{c}\bullet + \bullet\hat{c}^\dagger - \text{Tr}[\hat{c}\bullet + \bullet\hat{c}^\dagger]\bullet$ and ΔW is the Wiener increment with zero mean and Δt variance [12]. Averaging over the realizations of the Wiener increment gives $\rho(t + \Delta t) = \rho(t) + \Delta t \mathcal{D}[\hat{c}]\rho(t)$, to first-order in Δt , as given earlier in Eq. (13). Although the SMEs are not employed for unraveling quantum evolution in this work, we present their properties to provide a comprehensive comparison with other methods.

Conditions	Satisfaction		
	(C1) Complete positivity	(C2) Convex-linearity	(C3) Trace preservation
Method I	✓	✓	iff $\int dr \hat{K}_r^\dagger \hat{K}_r = \hat{1}$
Method II	✓	iff $\wp_{\mathbf{g}}(r \rho(t)) \propto \text{Tr}[\hat{K}_r \rho(t) \hat{K}_r^\dagger]$	✓
Av. SME	Errors at $\mathcal{O}(\Delta t^2)$	✓	✓

TABLE I. Summary of conditions for each method of valid average quantum evolution to satisfy (✓) the three conditions (C1)-(C3) in Fig. 1(b). We use “Av. SMEs” as a short hand for the averaged SME. Note that we have simplified the notation by using $\hat{K}_r \equiv \hat{K}(r)$.

Given all these different maps and methods to obtain average quantum evolutions, it is natural to ask which method is better when Δt is finite, when the Kraus operator is typically no longer exactly as Eq. (3) (or the SME is only first order in Δt). To address this question, a systematic criterion is needed to evaluate the validity of maps for the average evolution. We consider the three conditions (C1)-(C3) for valid average quantum evolution, as illustrated in the hierarchy diagram in Fig. 1(b). The three conditions, as summarized in Table I, are stated as follows:

Condition (C1) Complete Positivity. A map is completely positive when its acting on part of a bipartite quantum state is positive. That is: it maps a positive state to a positive state.

This condition is always satisfied for a map with Kraus operators, for instance, Method I and Method II, ensure complete positivity by construction. By contrast, the averaged SME in Eq. (13) may violate this condition beyond first order in Δt (see Appendix A for a detailed calculation).

Condition (C2) Convex-linearity. A map is convex-linear if a quantum state ρ is mapped to a quantum state which is convex-linear in ρ . That is: a weighted mixture of two states is mapped to the same-weight mixture of the individually mapped states.

Method I and the averaged SME always satisfy this condition. That is because, for Method I, the normalization factor is cancelled as in Eq. (18), leaving only the linear terms in ρ . For the averaged SME, the nonlinear term, $\mathcal{H}[\hat{c}]$, are also averaged out. Interestingly, Method II fulfills (C2) if and only if the guessed PDF exactly satisfies $\wp_{\mathbf{g}}(r|\rho(t)) \propto \text{Tr}[\hat{K}(r)\rho(t)\hat{K}^\dagger(r)]$, thus canceling the norm denominator in Eq. (19).

Condition (C3) Trace Preservation. A map is trace preserving if the trace of the mapped state is the same as that of the initial state.

Method II and the averaged SME always satisfy this condition. This is because, for Method II in Eq. (19), the map is always normalized by its trace. For the trace of the averaged SME, it is always one as $\text{Tr}[\mathcal{D}[\hat{c}]\rho]$ vanishes. However, for Method I, it satisfies this condition if and only if the completeness relation Eq. (8) holds exactly.

It is notable that the three conditions are independent as any one can fail for some method. In the next section, we take the reader through different approximations of Kraus operators that have been proposed in the literature. We will first examine Method I and II to explore the Lindblad condition (B) at high orders in Δt . The average evolution, as depicted in Table I, can be then used to assess the errors of conditions (C1)-(C3), depending on the method employed. For example, Method I, only the (C3) condition requires verification, while for Method II, only (C2) needs to be assessed. Finally, we investigate the validation of the quantum trajectory condition (A) by utilizing existing exact maps for the two qubit examples, which will be elaborated on in Section VI.

III. MEASUREMENT OPERATORS FROM EXISTING APPROACHES

In this section, we review the existing approaches proposed in the literature to show their satisfaction of conditions (C1)-(C3) at high-order in Δt for Method I and II. Their resulting average evolutions are also checked with the Lindblad evolution shown in Eq. (16), expanded up to the order of Δt^2 . We focus particularly on the homodyne detection, as an example of the diffusive-type measurements, which has been used in quantum optics [4, 16–19] and circuit quantum electrodynamics [35–38] experiments. Generalization to other diffusive measurements such as the heterodyne is quite straightforward. The conditioned state dynamics from these measurements resemble diffusive stochastic processes, as the noise in the records are Gaussian white noises in the continuous-in-time limit.

In the following subsections, we start with constructing a general form of diffusive-type measurement operators, and then investigating an operator that leads to the Itô stochastic master equations (SMEs), the adapted version of the conventional (first-order) Itô approach by Rouchon and Ralph [33] using the Euler-Milstein method, and lastly the so-called completely-positive trajectory method proposed by Guevara and Wiseman [43]. For simplicity, we will again only consider the situation of a single Lindblad operator \hat{c} , and take the system's interaction-frame Hamiltonian to be $\hat{H} = 0$.

A. Constructing measurement operators for diffusive measurement

Let us start with constructing a general form of measurement operators following Eq. (3), for a quantum system undergoing a time-continuous homodyne measurement. As is standard, we assume the quantum system (e.g., a qubit) is coupled to a Markovian bosonic field. The interaction Hamiltonian in the rotating-wave approximation is given by $\hat{V}_t = -i[\hat{c}d\hat{B}_t^\dagger - \hat{c}^\dagger d\hat{B}_t]$ [5, 18, 53, 54], where $d\hat{B}_t$ is an infinitesimal operator for the bath excitation. The evolution of the system-bath's state, for an infinitesimal time dt , is then described by a coupling unitary operator,

$$\hat{U}_{t+dt,t} = \exp[\hat{c}d\hat{B}_t^\dagger - \hat{c}^\dagger d\hat{B}_t]. \quad (21)$$

The operator $d\hat{B}_t$ has the following commutator relation:

$$[d\hat{B}_t, d\hat{B}_t^\dagger] = dt, \quad (22)$$

whence one can see that $d\hat{B}_t d\hat{B}_t^\dagger = \mathcal{O}(dt)$. This is consistent with defining annihilation and creation operators on a piece of field of duration dt by $d\hat{B}_t|n\rangle = \sqrt{dt}n|n-1\rangle$ and $d\hat{B}_t^\dagger|n\rangle = \sqrt{dt(n+1)}|n+1\rangle$, respectively. The commutator relation in Eq. (22) will be useful in keeping orders of the expansion later.

Now that we have the general form of the unitary operator in the interaction frame, we can calculate the system's evolution conditioned on the bath state being measured. We assume the bath initial state is in a vacuum state, i.e., $d\hat{B}_t|0\rangle = 0$ for all t . After the interaction with the system via the unitary operator Eq. (21), the bath's state is then observed via a homodyne measurement. The homodyne measurement gives information about a bath's quadrature denoted by $\hat{Q}_t = d\hat{B}_t + d\hat{B}_t^\dagger$. Therefore, given a measurement readout y_s collected during an instantaneous time between $t = s$ and $t = s + dt$, the homodyne measurement projects the bath's state onto an eigenstate of the quadrature, i.e., $\hat{Q}_s|y_s\rangle = y_s|y_s\rangle$. This eigenstate is simply the spatial coordinate of a Harmonic oscillator. One can write a Fock state $|n\rangle$ in this basis as a normalized wavefunction

$$\langle y_s|n\rangle = \frac{(\alpha/\pi)^{1/4}}{\sqrt{2^n n!}} \exp(-\alpha y_s^2/2) H_n(\sqrt{\alpha} y_s), \quad (23)$$

where $\alpha = dt/2$ and H_n are the Hermite polynomials for non-negative integers n .

Following the definition of the Kraus operator in Eq. (3) and the unitary operator in Eq. (21), the form of measurement operators is given by

$$\hat{K}(y_s) = \langle y_s| \exp[\hat{c}d\hat{B}_t^\dagger - \hat{c}^\dagger d\hat{B}_t] |0\rangle, \quad (24)$$

which is not simple to compute exactly. From the commutation relation in Eq. (22), we know that $d\hat{B}_t d\hat{B}_t^\dagger = \mathcal{O}(dt)$ in Eq. 24. Therefore, one can expand the exponential function and keep terms only to some orders in

$d\hat{B}_t$ and $d\hat{B}_t^\dagger$. For continuous measurement, we must at least keep terms up to first order in dt , which are terms with $d\hat{B}_t^2$, $d\hat{B}_t d\hat{B}_t^\dagger$, and $(d\hat{B}_t^\dagger)^2$. Let us define a big- \mathcal{O} notation for the bath operator, $\mathcal{O}[[d\hat{B}_t]^n]$, for any polynomial in $d\hat{B}_t$ and $d\hat{B}_t^\dagger$ of degree up to n . For $n = 2$, the expansion then gives

$$\begin{aligned} \hat{K}(y_s) &= \langle y_s | \hat{1} + \hat{c} d\hat{B}_t^\dagger - \frac{1}{2} \hat{c}^\dagger \hat{c} d\hat{B}_t d\hat{B}_t^\dagger + \frac{1}{2} \hat{c}^2 (d\hat{B}_t^\dagger)^2 \\ &\quad + \mathcal{O}[[d\hat{B}_t]^3] | 0 \rangle, \\ &= \langle y_s | 0 \rangle \left[\hat{1} - \frac{1}{2} \hat{c}^\dagger \hat{c} dt + \hat{c} y_s dt + \frac{1}{2} \hat{c}^2 (y_s^2 dt^2 - dt), \right. \\ &\quad \left. + \mathcal{O}(dt^{3/2}) \right] \\ &\equiv \hat{K}_1(y_s) + \mathcal{O}(dt^{3/2}), \end{aligned} \quad (25)$$

where we have already used the annihilation and creation properties of the bath operator $d\hat{B}_t$, and the wavefunction in Eq. (23). Note that $\hat{K}_1(y_s)$ is defined to represent terms with the dimension of the first order in Δt . In Eq. (25), we have also separated out a common term $\langle y_s | 0 \rangle$ so that the measurement operator is of the form

$$\hat{K}(y_s) = \sqrt{\wp_{\text{ost}}(y_s)} \hat{M}(y_s), \quad (26)$$

where we have defined an *ostensible probability*

$$\wp_{\text{ost}}(y_s) = |\langle y_s | 0 \rangle|^2 = \left(\frac{dt}{2\pi} \right)^{1/2} \exp(-y_s^2 dt/2), \quad (27)$$

and an *unnormalized measurement operator*

$$\hat{M}(y_s) = \hat{1} - \frac{1}{2} \hat{c}^\dagger \hat{c} dt + \hat{c} y_s dt + \frac{1}{2} \hat{c}^2 (y_s^2 dt^2 - dt) + \mathcal{O}(dt^{3/2}), \quad (28)$$

which can be used in place of $\hat{K}(y_s)$, especially when the factor $\sqrt{\wp_{\text{ost}}(y_s)}$ is not needed, such as in the normalized map Eq. (4).

We note that the discussion in this section only applies when dt is an infinitesimal time increment, where the measurement result y_s is acquired from the detection during the time between $t = s$ and $t = s + dt$. However, as we mentioned in the introduction, it is impossible to implement an infinitesimal time resolution dt in a real experiment and one instead needs to consider a finite time resolution Δt . This brings us to defining a coarse-grained measurement record, where the measurement result are obtained from a system with finite correlation time or a finite-bandwidth detector. If Δt is chosen as the integration time, then the coarse-grained signal is typically of the form,

$$Y_t = \frac{1}{\Delta t} \int_t^{t+\Delta t} ds y_s, \quad (29)$$

which is a time average of the infinitesimal record y_s over the time Δt . For example, in superconducting qubit experiments [25, 34, 35], the integration time is carefully chosen to match cavity's decay rates (such that the Markovian assumption is still approximately valid), but still short enough compared to other time scales of the systems.

B. Conventional Itô approach

We first consider the conventional approach used in constructing Itô (diffusive) stochastic differential equation (SDE) for quantum trajectories [13–16, 55]. The treatment of the Itô SDE for the quantum optics setting can be found in Carmichael's work [4], with the derivation similar to that in the previous subsection, but with the Itô rule, i.e., approximating that $y_s^2 dt^2 \approx dt$ being applied for an infinitesimal measurement result y_s during an infinitesimal time dt . Therefore, the fourth term in Eq. (28) vanishes, leading to an operator, $\hat{M}(y_s) = \hat{1} - \frac{1}{2} \hat{c}^\dagger \hat{c} dt + \hat{c} y_s dt$. For a finite time increment, one can simply replace dt with Δt and the record y_s with a coarse-grained record Y_t . However, one can also systematically derive what we call the Itô measurement operator for a finite time increment Δt . Let us discretize time to $m = \Delta t/dt$ infinitesimal time. We can compute a product of multiple $\hat{M}(y_s)$ defined for measurement records: $\{y_s : s \in \{t, t + dt, \dots, t + (m-1)dt\}\}$ and take the mean square limit to get (see Appendix B for the full derivation),

$$\hat{M}_I(Y_t) = \hat{1} - \frac{1}{2} \hat{c}^\dagger \hat{c} \Delta t + \hat{c} Y_t \Delta t, \quad (30)$$

where the subscript 'I' denotes 'Itô' and a normalized factor is found to be $\sqrt{\wp_{\text{ost}}(Y_t)}$ given a new ostensible probability

$$\wp_{\text{ost}}(Y_t) = \left(\frac{\Delta t}{2\pi} \right)^{1/2} \exp(-Y_t^2 \Delta t/2). \quad (31)$$

This Itô measurement operator is the most used approach in the literature, especially in theoretical work related to continuous quantum measurement. However, as we show in the following, whenever Δt is finite, this map satisfies the conditions (C1)-(C3) only to the first order in Δt . Errors of order Δt^2 turn out to depend on the methods (Method I and II) we use to calculate the average, as we now show.

1. Itô approach Method I: Linear

From Table I, we only need to check the conditions (B) and (C3), as (C1) and (C2) are already satisfied. Given the measurement operator and its ostensible probability in Eqs. (30) and (31), we obtain the Kraus operator for the Itô approach

$$\hat{K}_I(Y_t) = \sqrt{\wp_{\text{ost}}(Y_t)} \hat{M}_I(Y_t), \quad (32)$$

which can be used to compute a readout's PDF following the definition in Eq. (5),

$$\wp_{I,k}(Y_t | \rho(t)) = \wp_{\text{ost}}(Y_t) \text{Tr} \left\{ \mathcal{J}[\hat{M}_I(Y_t)] \rho(t) \right\}, \quad (33)$$

where the superoperator $\mathcal{J}[\bullet]$ was defined in Eq. (2) and $\wp_{I,k}$ is the PDF derived from the Kraus operator.

One can use this PDF to compute the average dynamics following the third line of Eq. (16). By substituting $\hat{M}_I(Y_t)$ from Eq. (30), expanding terms, and integrating over Y_t with the ostensible probability $\wp_{\text{ost}}(Y_t)$, keeping only terms up to $\mathcal{O}(\Delta t^2)$, we obtain

$$\begin{aligned} \rho(t + \Delta t) &= \int dY_t \wp_{\text{ost}}(Y_t) \hat{M}_I(Y_t) \rho(t) \hat{M}_I^\dagger(Y_t) \\ &= \rho(t) + \mathcal{D}[\hat{c}] \rho(t) \Delta t + \frac{1}{4} \hat{c}^\dagger \hat{c} \rho(t) \hat{c}^\dagger \hat{c} \Delta t^2. \end{aligned} \quad (34)$$

We can see that the resulting average dynamics agrees with the Lindblad evolution Eq. (14), to only first order in Δt , while the $\mathcal{O}(\Delta t^2)$ term is just a part of the double Lindblad operator Eq. (15).

Even though the average dynamics Eq. (34) is linear in $\rho(t)$ to second order in Δt , the trace-preserving condition (C3) of the Itô measurement operator is only satisfied to the first order in Δt . This can be verified via the completeness condition in Eq. (8). Since we have the Kraus-form operator, we can directly compute the completeness condition as,

$$\int dY_t \wp_{\text{ost}}(Y_t) \hat{M}_I^\dagger(Y_t) \hat{M}_I(Y_t) = \hat{1} + \frac{1}{4} (\hat{c}^\dagger \hat{c})^2 \Delta t^2, \quad (35)$$

which turns out to have a term of the order $\mathcal{O}(\Delta t^2)$ in addition to the identity. In other words, from Eq. (35), we show that the Itô measurement operator $\hat{M}_I(Y_t)$ is only trace preserving (C3) to first order in Δt .

2. Itô approach Method II: Nonlinear

The above violation of trace-preservation of the linear Itô approach — which is needed for purposes such as quantum state smoothing — is not typically an issue with quantum state filtering. That is because this can be treated using a nonlinear, exactly trace-preserving, method. Here the standard implementation of this Itô approach is to approximate the readout's PDF as Gaussian, where the readout can be written as a sum of its informative and noisy parts,

$$Y_t \Delta t = \mu_I \Delta t + \Delta W_I. \quad (36)$$

Here ΔW_I is the well-known zero-mean Wiener increment and μ_I is the mean readout. In order to find a consistent μ_I and verify the moments of ΔW_I , one can use Eq. (33) and Eq. (36) to show that

$$\mu_I = \langle \hat{c} + \hat{c}^\dagger \rangle + \mathcal{O}(\Delta t), \quad (37)$$

$$\sigma_I^2 = 1/\Delta t + \mathcal{O}(\Delta t^0), \quad (38)$$

following the definitions of μ and σ in Eqs. (6a) and (6b), using the notation $\langle \bullet \rangle \equiv \text{Tr}[\bullet \rho(t)]$ and keeping terms to lowest order in Δt . We can also verify that

$$\text{E}\{\Delta W_I\} = 0, \quad (39a)$$

$$\text{E}\{\Delta W_I^2\} = \Delta t, \quad (39b)$$

$$\text{E}\{\Delta W_I^4\} = 3\Delta t^2, \quad (39c)$$

describing statistics of the Wiener process. Therefore, we can approximate the readout's PDF as a Gaussian distribution with the mean μ_I and variance σ_I , i.e.,

$$\wp_{\text{I,g}}(Y_t | \rho(t)) = \left(\frac{\Delta t}{2\pi} \right)^{1/2} \exp \left[- (Y_t - \langle \hat{c} + \hat{c}^\dagger \rangle)^2 \Delta t / 2 \right]. \quad (40)$$

It is interesting to note that this guessed PDF is different from the PDF from Kraus operators, $\wp_{\text{I,k}}(Y_t | \rho(t))$ in Eq. (33).

From Table I, we only need to verify the conditions (B) and (C2). Using the Gaussian-approximated PDF of Y_t and the statistical moments of ΔW_I above, we can show that the average (unconditioned) quantum trajectory, following the second line of Eq. (16), gives a different result from the previous case to second order in Δt . By expanding the conditioned state, $\tilde{\mathcal{J}}[\hat{M}_I(Y_t)] \rho(t)$ in Eq. (16), keeping terms of the order Δt^2 and ΔW_I^4 , writing Y_t in terms of ΔW_I , and adopting the moments of ΔW_I in Eqs. (39), we get:

$$\begin{aligned} \rho(t + \Delta t) &= \text{E}\{\tilde{\mathcal{J}}[\hat{M}_I(Y_t)] \rho(t)\} \\ &= \rho(t) + \mathcal{D}[\hat{c}] \rho(t) \Delta t + \left[\frac{1}{4} \hat{c}^\dagger \hat{c} \rho(t) \hat{c}^\dagger \hat{c} \right. \\ &\quad + \hat{c} \rho(t) \hat{c}^\dagger (\langle \hat{c} + \hat{c}^\dagger \rangle^2 - 2\langle \hat{c}^\dagger \hat{c} \rangle) \\ &\quad + \rho(t) (2\langle \hat{c}^\dagger \hat{c} \rangle^2 + 3\langle \hat{c}^\dagger \hat{c} \rangle \langle \hat{c} + \hat{c}^\dagger \rangle^2 - \frac{1}{2} \langle \hat{c}^\dagger \hat{c}^2 \\ &\quad + (\hat{c}^\dagger)^2 \hat{c} \rangle \langle \hat{c} + \hat{c}^\dagger \rangle - \frac{1}{4} \langle (\hat{c}^\dagger \hat{c})^2 \rangle + \langle \hat{c} + \hat{c}^\dagger \rangle^4) \\ &\quad - [\rho(t) \hat{c}^\dagger + \hat{c} \rho(t)] (\langle -\hat{c} + \hat{c}^\dagger \rangle^3 + 2\langle \hat{c} + \hat{c}^\dagger \rangle \langle \hat{c}^\dagger \hat{c} \rangle \\ &\quad \left. + \frac{1}{2} \langle \hat{c}^\dagger \hat{c}^2 + (\hat{c}^\dagger)^2 \hat{c} \rangle \right] \Delta t^2 + \mathcal{O}(\Delta t^3). \end{aligned} \quad (41)$$

Once again, it is seen that this unconditioned evolution only aligns with the Lindblad evolution (B) to the first order in Δt . For the convex-linearity (C2), we can infer from Eq. (41) that its right-hand side is nonlinear in ρ for terms of order Δt^2 . The nonlinear terms arise from the trace of the dominator, which is $\text{Tr}[\mathcal{J}[\hat{M}_I(Y_t)] \rho(t)] \neq 1$ even if $\text{Tr}[\rho(t)] = 1$. Thus, the condition (C2) for the Itô map is satisfied only to the first order in Δt .

C. Rouchon-Ralph approach

Let us move on to the next existing approach, an extended version of the Itô approach. Proposed by Rouchon and Ralph [33] as a more efficient quantum filtering for continuous weak measurement, it is based on the Euler-Milstein stochastic simulation method [42]. The proposed technique makes the stochastic increment strongly convergent to first order in Δt as opposed to the conventional Itô approach, which is weakly convergent to Δt [33]. Following the notation used in the previous subsection for the single Lindblad operator \hat{c} and assuming that the technique can be used with the coarse-grained measurement record Y_t , we write the Rouchon-Ralph

measurement operator as

$$\hat{M}_R(Y_t) = \hat{1} - \frac{1}{2}\hat{c}^\dagger\hat{c}\Delta t + \hat{c}Y_t\Delta t - \frac{1}{2}\hat{c}^2(\Delta t - Y_t^2\Delta t^2), \quad (42)$$

where the last term is an addition to the Itô measurement operator, Eq. (30). This term corresponds to the correction following the Euler-Milstein method and will vanish if one naively applies the Itô rule, i.e., $Y_t^2\Delta t^2 \approx \Delta t$, making $\hat{M}_R \approx \hat{M}_I$. It is also interesting to note that, what we call, the Rouchon-Ralph (RR) operator, Eq. (42), can be alternatively derived from the interaction unitary operator as described in Section III A, using Eqs. (25) and (28), where all terms up to the order $\mathcal{O}(dt^{3/2})$ are included (also replacing dt and y_s with Δt and Y_t , respectively). In the following subsections, similar to the analyses in the Itô case, we present the two ways of writing the readout's PDF used in computing the average trajectory and its properties, and show how this RR map satisfy the hierarchy conditions.

1. RR approach Method I: Linear

Given the unnormalized measurement operator \hat{M}_R in Eq. (42) and the ostensible probability in Eq. (31) as in the Itô case, the Kraus operator for the Rouchon-Ralph (RR) approach is written as

$$\hat{K}_R(Y_t) = \sqrt{\wp_{\text{ost}}(Y_t)}\hat{M}_R(Y_t), \quad (43)$$

which, following the definition of the readout's PDF in Eq. (5), leads to

$$\wp_{R,k}(Y_t|\rho(t)) = \wp_{\text{ost}}(Y_t)\text{Tr}\{\mathcal{J}[\hat{M}_R(Y_t)]\rho(t)\}. \quad (44)$$

As before, we can compute the average unconditioned dynamics to second order in Δt to obtain

$$\begin{aligned} \rho(t + \Delta t) &= \int dY_t \wp_{\text{ost}}(Y_t) \hat{M}_R(Y_t) \rho(t) \hat{M}_R^\dagger(Y_t) \\ &= \rho(t) + \mathcal{D}[\hat{c}]\rho(t)\Delta t \\ &\quad + \left[\frac{1}{4}\hat{c}^\dagger\hat{c}\rho(t)\hat{c}^\dagger\hat{c} + \frac{1}{2}\hat{c}^2\rho(t)(\hat{c}^\dagger)^2\right]\Delta t^2 + \mathcal{O}(\Delta t^3), \end{aligned} \quad (45)$$

which only agrees with the Lindblad evolution (B) in Eq. (14) only to first order in Δt . For the trace-preserving condition (C3), we compute the completeness relation in Eq. (8), and find that

$$\begin{aligned} \int dY_t \wp_{\text{ost}}(Y_t) \hat{M}_R^\dagger(Y_t) \hat{M}_R(Y_t) \\ = \hat{1} + \left[\frac{1}{4}(\hat{c}^\dagger\hat{c})^2 + \frac{1}{2}(\hat{c}^\dagger)^2\hat{c}^2\right]\Delta t^2 + \mathcal{O}(\Delta t^3), \end{aligned} \quad (46)$$

which shows that the RR measurement operator satisfies (C3) only to first order in Δt , same as for the Itô case. Interestingly, even though there is an extra positive term of $\mathcal{O}(\Delta t^2)$ in the completeness condition, beyond the standard Itô case in Eq. (35), we will see later in Section VI that this approach results in a slight improvement in estimating individual trajectories compared to the original Itô approach.

2. RR approach Method II: Nonlinear

In the work by Rouchon and Ralph [33] and the one from Rouchon works [41], they preferred using the Gaussian approximation for the measurement readout's PDF, where the measurement readout was written as

$$Y_t\Delta t = \mu_R\Delta t + \Delta W_R, \quad (47)$$

where the statistical properties of ΔW_R are exactly those of ΔW_I in Eqs. (39). Using these statistics, we compute the average evolution from Eq. (16) and get

$$\begin{aligned} \rho(t + \Delta t) &= \text{E}\{\tilde{\mathcal{J}}[\hat{M}_R(Y_t)]\rho(t)\}, \\ &= \text{E}\{\tilde{\mathcal{J}}[\hat{M}_I(Y_t)]\rho(t)\} + \left[\frac{1}{2}\hat{c}^2\rho(t)(\hat{c}^\dagger)^2\right. \\ &\quad + \rho(t)\left(-\frac{1}{2}\langle\hat{c}^2(\hat{c}^\dagger)^2\rangle - \frac{1}{2}\langle\hat{c}^2 + (\hat{c}^\dagger)^2\rangle\langle\hat{c}^\dagger + \hat{c}\rangle^2\right. \\ &\quad \left. - \langle(\hat{c}^\dagger)^2\hat{c} + \hat{c}^\dagger\hat{c}^2\rangle\langle\hat{c} + \hat{c}^\dagger\rangle + \frac{1}{2}\langle\hat{c}^2 + (\hat{c}^\dagger)^2\rangle^2\right) \\ &\quad + [\rho(t)\hat{c}^\dagger + \hat{c}\rho(t)]\left(-\langle\hat{c}^2 + (\hat{c}^\dagger)^2\rangle\langle\hat{c} + \hat{c}^\dagger\rangle\right. \\ &\quad \left. - \langle\hat{c}^\dagger\hat{c}^2 + (\hat{c}^\dagger)^2\hat{c}\rangle - \hat{c}\rho(t)\hat{c}^\dagger\langle\hat{c}^2 + (\hat{c}^\dagger)^2\rangle\right) \\ &\quad + [\hat{c}^2\rho(t) + \rho(t)(\hat{c}^\dagger)^2]\left(\frac{1}{2}\langle\hat{c} + \hat{c}^\dagger\rangle^2\right. \\ &\quad \left. - \frac{1}{2}\langle\hat{c}^2 + (\hat{c}^\dagger)^2\rangle - \langle\hat{c}^\dagger\hat{c}\rangle\right)]\Delta t^2 + \mathcal{O}(\Delta t^3), \end{aligned} \quad (48)$$

where we can see that, again, the result only agrees with Lindblad evolution (B) to first order in Δt , same as in the Itô case. We note that the error terms of order $\mathcal{O}(\Delta t^2)$ from Method I Eq. (45) and Method II Eq. (48) are different from each other. Moreover, one can see that the non convex-linear in $\rho(t)$ terms appear in $\mathcal{O}(\Delta t^2)$, failing to satisfy the condition (C2) at $\mathcal{O}(\Delta t^2)$.

D. Guevara-Wiseman approach

The last existing approach we consider is that introduced by Guevara and Wiseman [43]. Since the Itô map satisfies the complete positivity only to first order in Δt , they considered adding extra terms to the measurement operator such that it would satisfy the completeness relation to the order of Δt^2 . Their so-called complete positivity map for quantum trajectories was proposed for both jumps and diffusive measurement records and was implemented in the quantum state smoothing [48, 56]. Using our notation for consistency, the Guevara-Wiseman measurement operator for a single Lindblad channel \hat{c} and the coarse-grained record is given by

$$\hat{M}_G(Y_t) = \hat{1} + (Y_t\hat{c} - \frac{1}{2}\hat{c}^\dagger\hat{c})\Delta t - \frac{1}{8}(\hat{c}^\dagger\hat{c})^2\Delta t^2. \quad (49)$$

We note that this operator has one extra term, $-\frac{1}{8}(\hat{c}^\dagger\hat{c})^2\Delta t^2$, in addition to the Itô operator. This extra term was proposed as a correction term, in order to remove the non-zero term in the second order in Δt in the Itô completeness condition Eq. (35). As before, we compare the properties of the operator computed from two methods.

1. GW approach Method I: Linear

We follow the original derivation in Ref. [43] and use the operator \hat{M}_G in Eq. (49) and its ostensible probability in Eq. (31) to construct the Kraus operator for the Guevara-Wiseman (GW) approach

$$\hat{K}_G(Y_t) = \sqrt{\wp_{\text{ost}}(Y_t)} \hat{M}_G(Y_t) \quad (50)$$

which leads to the readout's PDF as

$$\wp_{G,k}(Y_t|\rho(t)) = \wp_{\text{ost}}(Y_t) \text{Tr} \{ \mathcal{J}[\hat{M}_G(Y_t)]\rho(t) \}. \quad (51)$$

Using the above to compute the average dynamics to second order in Δt , we obtain

$$\begin{aligned} \rho(t + \Delta t) &= \int dY_t \wp_{\text{ost}}(Y_t) \hat{M}_G(Y_t) \rho(t) \hat{M}_G^\dagger(Y_t) \\ &= \rho(t) + \mathcal{D}[\hat{c}]\rho(t)\Delta t + \frac{1}{4}\mathcal{D}[\hat{c}^\dagger\hat{c}]\rho(t)\Delta t^2 + \mathcal{O}(\Delta t^3). \end{aligned} \quad (52)$$

We can see that, the average dynamics still only match with the exact Lindblad evolution (B), in Eq. (14) to the first order in Δt . However, for the completeness condition, we have

$$\int dY_t \wp_{\text{ost}}(Y_t) \hat{M}_G^\dagger(Y_t) \hat{M}_G(Y_t) = \hat{1} + \mathcal{O}(\Delta t^3), \quad (53)$$

which confirms the purpose of GW measurement operator that it should be trace preserving (C3) to second order in Δt , better than in the previous two approaches.

2. GW approach Method II: Nonlinear

In the original proposal Ref. [43], the authors also suggested a consistent way to approximate the readout's PDF as a Gaussian distribution that has the same statistics as the PDF in Eq. (51) to second order in Δt . In order to achieve that, the mean and the variance of the Gaussian distribution have to be modified. Similarly to before, let us assume

$$Y_t \Delta t = \mu_G \Delta t + \Delta W_G, \quad (54)$$

we can now compute the modified mean and variance using Eq. (51) to get

$$\begin{aligned} \mu_G &= \langle \hat{c} + \hat{c}^\dagger \rangle - \frac{1}{2} \langle \hat{c}^\dagger \hat{c}^2 + \hat{c}(\hat{c}^\dagger)^2 \rangle \Delta t + \mathcal{O}(\Delta t^2), \\ \sigma_G^2 &= \frac{1}{\Delta t} + [2\langle \hat{c}^\dagger \hat{c} \rangle - \langle \hat{c}^\dagger + \hat{c} \rangle^2] + \mathcal{O}(\Delta t), \end{aligned} \quad (55)$$

noting that there were typos in the original paper Ref. [43] which should be replaced by our new calculations. We can also compute the new statistics of ΔW_G from Eq. (51), which gives

$$\begin{aligned} \text{E}\{\Delta W_G\} &= \text{E}\{\Delta W_G^3\} = 0, \\ \text{E}\{\Delta W_G^2\} &= \Delta t + (2\langle \hat{c}^\dagger \hat{c} \rangle - \langle \hat{c}^\dagger + \hat{c} \rangle^2) \Delta t^2 + \mathcal{O}(\Delta t^3), \\ \text{E}\{\Delta W_G^4\} &= 3\Delta t^2 + \mathcal{O}(\Delta t^3). \end{aligned} \quad (56)$$

These moments are consistent with a Gaussian distribution, with a higher-order correction to the variance compared to the standard Itô ΔW_1 . We can use the above properties to compute the average dynamics, i.e.,

$$\begin{aligned} \rho(t + \Delta t) &= \text{E}\{ \tilde{\mathcal{J}}[\hat{M}_G(Y_t)]\rho(t) \}, \\ &= \rho(t) + \mathcal{D}[\hat{c}]\rho(t)\Delta t + \frac{1}{4}\mathcal{D}[\hat{c}^\dagger\hat{c}]\rho(t)\Delta t^2 + \mathcal{O}(\Delta t^3), \end{aligned} \quad (57)$$

which exactly coincides with Eq. (52) using the PDF from the Kraus operator. Despite failing to agree with high-order Lindblad evolution, this measurement operator ensures the convex-linearity condition (C2) to $\mathcal{O}(\Delta t^2)$. Since (C1) and (C2) are automatically satisfied (see Table. I), this means that the GW-map \hat{M}_G generates valid average quantum evolution correct to $\mathcal{O}(\Delta t^2)$.

IV. CONSTRUCTING HIGH-ORDER COMPLETELY POSITIVE MAP

We have shown in the previous section that none of the existing approaches, even with two different ways of computing the readout's average, gives a perfect agreement with the Lindblad evolution (B) and two of them fail to generate valid average quantum evolution (C), to orders higher than Δt . In this section, we propose a measurement operator that satisfy all conditions (B) and (C1)-(C3) to second order in Δt . We derive such operator based on series expansion of the exact Kraus operator in Eq. (24). Similar to other approaches, we only focus on the case with a single Lindblad channel and $\hat{H} = 0$ for simplicity.

Let us consider the exact Kraus operator and its expansion in Eqs. (24) and (25), but now keep terms from its expansion to $\mathcal{O}[[d\hat{B}_t]^4]$. As before, using the annihilation and creation properties of the bath operator $d\hat{B}_t$ and the wavefunction in Eq. (23), we obtain a high-order measurement operator denoted as $\hat{M}_2(y_s)$ for an infinitesimal measurement results y_s , where its full form is presented in Appendix C. We then follow an approach similar to that of Eq. (30), deriving a map for a finite Δt by discretizing time into $m = \Delta t/dt$ segments, multiplying $\hat{M}_2(y_s)$ m times, and taking limit $m \rightarrow \infty$ (see Appendix C for more detail). This yields our proposed coarse-grained operator $\hat{M}_W(Y_t)$ for a finite Δt as

$$\begin{aligned} \hat{M}_W(Y_t) &= \hat{1} - \frac{1}{2}(\hat{c}^2 + \hat{c}^\dagger\hat{c})\Delta t + \frac{1}{8}(\hat{c}^\dagger\hat{c})^2\Delta t^2 \\ &\quad + [\hat{c}\Delta t - \frac{1}{4}(\hat{c}^\dagger\hat{c}^2 + \hat{c}\hat{c}^\dagger\hat{c})\Delta t^2]Y_t + \frac{1}{2}\hat{c}^2\Delta t^2Y_t^2. \end{aligned} \quad (58)$$

This is one of our main results in this work. We see that our operator can be written in terms of the RR operator, $\hat{M}_R(Y_t)$ in Eq. (42), with three additional (high-order) terms: $\hat{M}_W(Y_t) = \hat{M}_R(Y_t) + \frac{1}{8}(\hat{c}^\dagger\hat{c})^2\Delta t^2 - \frac{1}{4}(\hat{c}^\dagger\hat{c}^2 + \hat{c}\hat{c}^\dagger\hat{c})\Delta t^2Y_t$. As we show in the following, we can use this high-order Kraus operator with two types of the readout's PDF to give the same average dynamics, and satisfying the conditions (B) and (C) to second order in Δt .

1. Higher-order approach Method I: Linear

Following the similar manner as in the existing approaches, using the operator in Eq. (58) and the ostensible probability in Eq. (31), we can write the Kraus operator for our high-order approach as

$$\hat{K}_W(Y_t) = \sqrt{\wp_{\text{ost}}(Y_t)} \hat{M}_W(Y_t), \quad (59)$$

which leads to the readout's PDF,

$$\wp_{W,k}(Y_t|\rho(t)) = \wp_{\text{ost}}(Y_t) \text{Tr} \{ \mathcal{J}[\hat{M}_W(Y_t)]\rho(t) \}. \quad (60)$$

Using this PDF, we compute the average dynamics to the second order in Δt and find that

$$\begin{aligned} \rho(t + \Delta t) &= \int dY_t \wp_{\text{ost}}(Y_t) \hat{M}_W(Y_t) \rho(t) \hat{M}_W^\dagger(Y_t) \\ &= \rho(t) + \mathcal{D}[\hat{c}]\rho(t)\Delta t + \frac{1}{2}\mathcal{D}^2[\hat{c}]\rho(t)\Delta t^2 + \mathcal{O}(\Delta t^3), \end{aligned} \quad (61)$$

the average dynamics now are convex-linear and match exactly with the Lindblad solution (B) in Eq. (14) to the second order in Δt . From the implication in Fig. 1(b), it follows that the condition (C) should be satisfied to the same order. Indeed we can show that

$$\int dY_t \wp_{\text{ost}}(Y_t) \hat{M}_W^\dagger(Y_t) \hat{M}_W(Y_t) = \hat{1} + \mathcal{O}(\Delta t^3), \quad (62)$$

or the trace preservation (C3) is also exactly satisfied to second order in Δt . We will reproduce this with the other (nonlinear) method in the next following.

2. Higher-order approach Method II: Nonlinear

As in the Guevara-Wiseman approach, we can approximate the readout's PDF as a Gaussian distribution, but still obtain the same readout's statistics as the PDF in Eq. (60) to the second order in Δt . Similarly to other approaches, the readout is of the form

$$Y_t \Delta t = \mu_W \Delta t + \Delta W_W, \quad (63)$$

where the modified average and variance of the readout are computed from Eq. (60), which give

$$\begin{aligned} \mu_W &= \langle \hat{c} + \hat{c}^\dagger \rangle + \frac{1}{4} \langle (\hat{c}^\dagger)^2 \hat{c} + \hat{c}^\dagger \hat{c}^2 - \hat{c} \hat{c}^\dagger \hat{c} - \hat{c}^\dagger \hat{c} \hat{c}^\dagger \rangle \Delta t + \mathcal{O}(\Delta t^2), \\ \sigma_W^2 &= \frac{1}{\Delta t} + \left[2 \langle \hat{c}^\dagger \hat{c} \rangle - \langle \hat{c}^\dagger + \hat{c} \rangle^2 + \langle \hat{c}^2 + (\hat{c}^\dagger)^2 \rangle \right] \Delta t. \end{aligned} \quad (64)$$

We also find that the innovation ΔW_W has the consistent ensemble-average properties:

$$\begin{aligned} \text{E}\{\Delta W_W\} &= \text{E}\{\Delta W_W^3\} = 0, \\ \text{E}\{\Delta W_W^2\} &= \Delta t + \left[2 \langle \hat{c}^\dagger \hat{c} \rangle - \langle \hat{c}^\dagger + \hat{c} \rangle^2 + \langle \hat{c}^2 + (\hat{c}^\dagger)^2 \rangle \right] \Delta t^2, \\ \text{E}\{\Delta W_W^4\} &= 3\Delta t^2. \end{aligned} \quad (65)$$

Therefore, using the above properties, we can derive the average dynamics from

$$\begin{aligned} \rho(t + \Delta t) &= \text{E}\{ \tilde{\mathcal{J}}[\hat{M}_W(Y_t)]\rho(t) \}, \\ &= \rho(t) + \mathcal{D}[\hat{c}]\rho(t)\Delta t + \frac{1}{2}\mathcal{D}^2[\hat{c}]\rho(t)\Delta t^2 + \mathcal{O}(\Delta t^3), \end{aligned} \quad (66)$$

which is exactly equal to Eq. (61). We have shown that, again, the proposed high-order operator Eq. (58) results in the average evolution in perfect agreement with the Lindblad solution (B) and satisfy the conditions (C1)-(C3) to second order in Δt .

V. QUBIT EXAMPLE WITH EXACT MAPS

The proposed map has demonstrated high accuracy in generating average evolutions. The next natural question that arises is how accurate it is at the level of the conditioned (trajectory) evolution. In order to address the question, one needs an exact quantum trajectory as a benchmark. Here, we consider two examples of qubit measurement for which the conditioned trajectories can be solved exactly (or to high order of accuracy). These are the qubit z -measurement (Hermitian measurement, $\hat{c} \propto \hat{\sigma}_z$) and the measurement of qubit's fluorescence (non-Hermitian measurement, $\hat{c} \propto \hat{\sigma}_-$). Both have already been tested on various architectures of superconducting qubit experiments [34–38, 57, 58]. In the following subsections, we derive corresponding “exact” Kraus operators for the two examples. We will use these operators as a benchmark for exact individual trajectories in Section VI.

A. Measurements with Hermitian Lindblad operators (e.g., z -measurement)

We begin by considering a weak continuous measurement of a Hermitian observable. Measurements using Hermitian Lindblad operators align with the traditional von Neumann concept of measurement with quantum observables, where post-measurement states collapse to eigenstates of the observables over time. These measurements can range from weak (imprecise) to strong (projective). The measurement operator for this case can be motivated by Bayesian inference and statistical principles. This technique was originally proposed for solid-state qubits, utilizing quantum dots and quantum point contacts as measurement devices [20, 21, 59, 60]. It has since been adopted in continuous quantum measurement applications in superconducting qubit experiments. In this subsection, we present the derivation for any observable $\hat{A} = \sum_j a_j |a_j\rangle\langle a_j|$, where $|a_j\rangle$ and a_j are eigenstates and their corresponding eigenvalues of the observable.

Since we consider the weak continuous measurement, an important assumption is the central limit theorem, where the statistics of imprecision can be described by

Gaussian distribution. Therefore, the probability distribution of a measurement readout Y_t , given that the state was in the eigenstate $|a_j\rangle$, is

$$\wp(Y_t|a_j) = \left(\frac{\gamma\Delta t}{\pi}\right)^{1/2} \exp\left[-\frac{\gamma}{2}\left(\frac{Y_t}{\sqrt{2\gamma}} - a_j\right)^2 \Delta t\right], \quad (67)$$

where the measurement record is scaled such that the PDF is a Gaussian function around the mean value a_j . We note that the coefficient γ will be later related to a coupling rate. Following the original idea in Ref. [20], one can write the Kraus operator for this Hermitian measurement as [23]

$$\hat{K}_H(Y_t) = \sum_j \sqrt{\wp(Y_t|a_j)} |a_j\rangle\langle a_j|, \quad (68)$$

which is a matrix with diagonal elements given by the square roots of the readout probability distribution. Using Eq. (5), the operator Eq. (68) trivially gives the probability of the measurement result,

$$\wp(Y_t|a_j) = \text{Tr}[\hat{K}_H(Y_t)|a_j\rangle\langle a_j|\hat{K}_H^\dagger(Y_t)], \quad (69)$$

which is the exact PDF as in Eq. (67).

We can show that this measurement operator gives the average dynamics agreeing with the Lindblad solution to infinite orders in Δt , by showing that

$$\begin{aligned} \rho(t + \Delta t) &= \text{E}\{\tilde{\mathcal{J}}[\hat{K}_H(Y_t)]\rho(t)\} \\ &= \int dY_t \hat{K}_H(Y_t)\rho(t)\hat{K}_H^\dagger(Y_t) \\ &= e^{\Delta t \mathcal{D}[\sqrt{\gamma/2}\hat{A}]}\rho(t), \end{aligned} \quad (70)$$

where the third line comes from the fact that \hat{K}_H and \hat{A} are both diagonal in the eigenstate basis $\{|a_j\rangle\}$. The coupling γ is defined in the Lindblad operator $\hat{c} = \sqrt{\gamma/2}\hat{A}$. Eq. (70) justifies that this set of Kraus operators reproduces the Lindblad evolution to infinite order of Δt . An example of measurements with Hermitian Lindblad operators is the qubit measurement in z -basis, where $\hat{A} = \hat{\sigma}_z$, with two eigenstates: $|a_{+1}\rangle = |e\rangle$ and $|a_{-1}\rangle = |g\rangle$, the excited and ground states of the qubit, respectively.

B. Measurement of qubit fluorescence

The second example is qubit fluorescence measurement, which examines the energy relaxation or the transition of states of a qubit, i.e., from its excited state $|e\rangle$ to ground state $|g\rangle$. This results in an emission of a photon at the energy difference between the two levels. The photon emitted from the system can be detected by a measurement device, which, in this work, we assume a homodyne measurement. This type of measurement corresponds to the Lindblad operator $\hat{c} \propto \hat{\sigma}_-$, which is a qubit's lowering operator, i.e., non-Hermitian measurement. For non-Hermitian Lindblad operators, there is no general exact form of measurement operators as in

Eq. (68), but we can derive one for a qubit case. In the following, we start with deriving the exact Kraus operator, which is in terms of a weighted readout integral. Then, for it to be useful in analytical calculation later, we need to make an approximation to obtain a ‘‘nearly exact’’ operator.

1. Qubit fluorescence measurement: Exact operator

The measurement operator for qubit fluorescence measurement for a finite time Δt can be derived analytically by integrating the differential equation, which describes how the operator changes in an infinitesimal time. Consider a time $s+ds$, where s is introduced as a dummy variable for time and ds is an infinitesimal time. An operator at $s+ds$ can be decomposed as $\hat{M}(s+ds) = \hat{M}(ds)\hat{M}(s)$. This leads to a differential equation for the operator,

$$d\hat{M} = \hat{M}(s+ds) - \hat{M}(s) = [\hat{M}(ds) - \hat{1}]\hat{M}(s), \quad (71)$$

Since ds is infinitesimal, we can replace $\hat{M}(ds)$ by the Itô operator in Eq. (30) as it should be exact up to first order in ds . We then use $\hat{c} = \sqrt{\gamma}\hat{\sigma}_-$ for the fluorescence measurement and show that the differential equation Eq. (71) becomes

$$\begin{pmatrix} dm_{00} & dm_{01} \\ dm_{10} & dm_{11} \end{pmatrix} = \begin{pmatrix} -\frac{1}{2}\gamma ds & 0 \\ \sqrt{\gamma}y_s ds & 0 \end{pmatrix} \begin{pmatrix} m_{00}(s) & m_{01}(s) \\ m_{10}(s) & m_{11}(s) \end{pmatrix}, \quad (72)$$

where we have used $m_{jk}(s)$ for $j, k \in \{0, 1\}$ as the four elements of the matrix $\hat{M}(s)$.

To obtain the operator for a finite-time Δt , each element in Eq. (72) should be integrated from a time of interest t to $t + \Delta t$, with an initial condition $\hat{M}(t=0) = \hat{1}$. Therefore, one obtains the exact (unnormalized) measurement operator for the fluorescence case as

$$\hat{M}_{F,\text{ex}}(X_t) = \begin{pmatrix} e^{-\gamma\Delta t/2} & 0 \\ \sqrt{\gamma}X_t & 1 \end{pmatrix}, \quad (73)$$

where

$$X_t \equiv \int_t^{t+\Delta t} e^{-\gamma s/2} y_s ds \quad (74)$$

is a weighted readout integral from time t to $t + \Delta t$. To construct the Kraus operator for this case, we need to find the ostensible probability $\wp_{\text{ost}}(X_t)$ such that

$$\hat{K}_{F,\text{ex}}(X_t) = \sqrt{\wp_{\text{ost}}(X_t)}\hat{M}_{F,\text{ex}}(X_t). \quad (75)$$

The probability can be obtained via a multi-variable integration of the ostensible probability, $\wp(y_s)$, for infinitesimal measurement results as defined in Eq. (27) (see Appendix D for the detailed derivation). First, we find that X_t has zero mean, i.e., $\text{E}\{X_t\} = 0$, which is expected as X_t is a linear combination of zero-mean Gaussian variables, y_s . Second, we find that the variance is given

by $\sigma_{X_t}^2 = \mathbb{E}\{X_t^2\} - \mathbb{E}\{X_t\}^2 = 2e^{-\gamma(t+\Delta t/2)} \sinh(\gamma\Delta t/2)/\gamma$. Thus, we can construct the ostensible probability for X_t as

$$\wp_{\text{ost}}(X_t) = \frac{1}{\sqrt{2\pi\sigma_{X_t}^2}} \exp[-X_t^2/(2\sigma_{X_t}^2)]. \quad (76)$$

The exact Kraus operator with $\wp_{\text{ost}}(X_t)$ above is not trivial for analytical calculations. This brings us to approximate the weighted readout integral X_t . In the previous work Refs. [57, 58], this integrated readout was approximated to $\sqrt{\gamma}X_t \approx \sqrt{\gamma}Y_t\Delta t$, which is a Taylor expansion of the exponential weight $e^{-\gamma s/2}$ to only the zeroth order in s (we show in Appendix E that the resulting map only satisfies the condition (B) to first order in Δt , which is lower than what we want). Therefore, in order to benchmark exact individual trajectories, we need a more accurate map, considering higher-order terms in s . This will be derived in the following.

2. Qubit fluorescence measurement: Nearly exact operator

To calculate errors in the quantum trajectory, it is sufficient to consider an approximated version that can still capture the statistics of measurement results to high orders in Δt . Let us first expand the exponential function in X_t in the integral of Eq. (74) to first order in s , i.e., $e^{-\gamma s/2} = 1 - \gamma s/2$. One can rearrange terms, giving

$$\begin{aligned} X_t &= \int_t^{t+\Delta t} e^{-\gamma s/2} y_s ds \\ &\approx \int_t^{t+\Delta t} \left[1 - \frac{\gamma}{2}(t + \frac{\Delta t}{2}) - \frac{\gamma}{2}(s - t - \frac{\Delta t}{2})\right] y_s ds \\ &= \left[1 - \frac{\gamma}{2}(t + \frac{\Delta t}{2})\right] Y_t \Delta t - \frac{\gamma}{2} Z_t, \end{aligned} \quad (77)$$

where Y_t is as defined in Eq. (29), and

$$Z_t \equiv \int_t^{t+\Delta t} \left[s - (t + \frac{\Delta t}{2})\right] y_s ds, \quad (78)$$

which is another integrated-record variable. We will show later in Appendix D that, by defining the new variable this way, Y_t and Z_t are statistically independent. The measurement operator thus reads

$$\hat{M}_{\text{F}}(Y_t, Z_t) = \begin{pmatrix} e^{-\gamma\Delta t/2} & 0 \\ \sqrt{\gamma}[1 - \frac{\gamma}{2}(t + \frac{\Delta t}{2})]Y_t\Delta t - \frac{\gamma^{3/2}}{2}Z_t & 1 \end{pmatrix}, \quad (79)$$

which will be used as a benchmark for generating quantum trajectories.

Since there are now two record variables, Y_t and Z_t , we need to, again, find their statistical properties and moments of their ostensible probabilities. With the first and second moments, we can evaluate PDF of the variable Z_t (see Appendix D for the detailed derivation of multi-variable integration). First, we find that Z_t has

zero mean, i.e., $\mathbb{E}\{Z_t\} = 0$. Next, the variance is given by $\mathbb{E}\{Z_t^2\} - \mathbb{E}\{Z_t\}^2 = \Delta t^3/12$. We can further show that the co-variance of Y_t and Z_t is zero, meaning that they are statistically independent, i.e., $\mathbb{E}\{Y_t Z_t\} = 0$. We therefore construct an ostensible probability for Z_t as

$$\wp_{\text{ost}}(Z_t) = \sqrt{\frac{6}{\pi\Delta t^3}} \exp(-6Z_t^2/\Delta t^3). \quad (80)$$

Notice that the variable Z_t has the dimension of $\Delta t^{3/2}$. The nearly-exact Kraus operator for the qubit's fluorescence measurement is thus

$$\hat{K}_{\text{F}}(Y_t, Z_t) = \sqrt{\wp_{\text{ost}}(Y_t)\wp_{\text{ost}}(Z_t)} \hat{M}_{\text{F}}(Y_t, Z_t), \quad (81)$$

using the ostensible probabilities defined in Eqs. (31) and (80). Note that these only depend on the time step Δt , so the ensemble of the records is easier to generate than using $\wp_{\text{ost}}(X_t)$. We will use this form of the Kraus operator for the analytical calculation in the next section.

VI. INDIVIDUAL QUANTUM TRAJECTORY COMPARISON

In this section, we use the two qubit examples from the previous section—the qubit z -measurement and the qubit fluorescence measurement—to investigate the valid quantum trajectory condition (A) for all measurement operators. We do this by examining how closely the individual trajectories they generate match the exact trajectories produced by the exact (and nearly exact) operators. To measure the closeness between any two quantum states, we use the trace distance and compute an average over all possible states and measurement records.

Consider how an arbitrary quantum state $\tilde{\rho}$ will change after one finite-time step Δt , where the finite-time (coarsed-grained) measurement result Y_t is obtained. Denoting an exact (or nearly exact) Kraus operator by $\hat{K}_{\text{ex}}(\tilde{Y}_t)$ for relevant record variables \tilde{Y}_t , which can be either Y_t for the qubit z -measurement Eq. (68) or $\{Y_t, Z_t\}$ for the qubit fluorescence in Eq. (81), we compute the benchmark conditioned quantum state as

$$\rho_{\text{ex}}(\tilde{Y}_t, \tilde{\rho}) = \frac{\hat{K}_{\text{ex}}(\tilde{Y}_t) \tilde{\rho} \hat{K}_{\text{ex}}^\dagger(\tilde{Y}_t)}{\text{Tr}[\hat{K}_{\text{ex}}(\tilde{Y}_t) \tilde{\rho} \hat{K}_{\text{ex}}^\dagger(\tilde{Y}_t)]}. \quad (82)$$

If one instead uses an operator of the four \hat{K}_{A} , where $\text{A} \in \{\text{I}, \text{R}, \text{G}, \text{W}\}$ defined in Eqs. (30), (42), (49) and (58), respectively, only the coarse-grained Y_t is measured and the conditioned state becomes

$$\rho_{\text{A}}(Y_t, \tilde{\rho}) = \frac{\hat{K}_{\text{A}}(Y_t) \tilde{\rho} \hat{K}_{\text{A}}^\dagger(Y_t)}{\text{Tr}[\hat{K}_{\text{A}}(Y_t) \tilde{\rho} \hat{K}_{\text{A}}^\dagger(Y_t)]}, \quad (83)$$

as different estimates of the exact state. Therefore, we define the average trace distance for an approach A,

$$D_{\text{A}} = \frac{1}{2} \int d\mu_{\text{H}}(\tilde{\rho}) \int d\tilde{Y}_t \wp_{\text{ex}}(\tilde{Y}_t|\tilde{\rho}) \text{Tr}|\rho_{\text{A}} - \rho_{\text{ex}}|. \quad (84)$$

Methods	Average trace distance compared to $\hat{K}_H(Y_t)$	Average trace distance compared to $\hat{K}_F(Y_t, Z_t)$
\hat{K}_I	$\frac{7\sqrt{\pi}}{48}(\gamma\Delta t)^{3/2} + \mathcal{O}(\Delta t^{5/2}) \approx 0.2585(\gamma\Delta t)^{3/2}$	$\frac{1}{2\sqrt{6\pi}}(\gamma\Delta t)^{3/2} + \mathcal{O}(\Delta t^{5/2}) \approx 0.1152(\gamma\Delta t)^{3/2}$
\hat{K}_R	$\frac{(1+e^3)\sqrt{\pi}}{12e^3}(\gamma\Delta t)^{3/2} + \mathcal{O}(\Delta t^{5/2}) \approx 0.1551(\gamma\Delta t)^{3/2}$	$\frac{1}{2\sqrt{6\pi}}(\gamma\Delta t)^{3/2} + \mathcal{O}(\Delta t^{5/2}) \approx 0.1152(\gamma\Delta t)^{3/2}$
\hat{K}_G	$\frac{7\sqrt{\pi}}{48}(\gamma\Delta t)^{3/2} + \mathcal{O}(\Delta t^{5/2}) \approx 0.2585(\gamma\Delta t)^{3/2}$	$\frac{1}{2\sqrt{6\pi}}(\gamma\Delta t)^{3/2} + \mathcal{O}(\Delta t^{5/2}) \approx 0.1152(\gamma\Delta t)^{3/2}$
\hat{K}_W	$\frac{(4+e^{3/2})\sqrt{\pi}}{48e^{3/2}}(\gamma\Delta t)^{3/2} + \mathcal{O}(\Delta t^{5/2}) \approx 0.0699(\gamma\Delta t)^{3/2}$	$\frac{1}{4\sqrt{6\pi}}(\gamma\Delta t)^{3/2} + \mathcal{O}(\Delta t^{5/2}) \approx 0.0576(\gamma\Delta t)^{3/2}$

TABLE II. Analytical results of the average trace distance integrated over all possible states and measurement results defined in Eq. (84) for the two examples: the qubit z -measurement (left column) and the qubit fluorescence measurement of qubit fluorescence (right column).

Note that the trace distance between the state $\rho_A = \rho_A(Y_t, \tilde{\rho})$ in Eq. (83) and the exact state $\rho_{\text{ex}} = \rho_{\text{ex}}(Y_t, \tilde{\rho})$ in Eq. (82) is averaged over the measurement results Y_t , with its probability weight computed from the exact measurement operator, $\wp_{\text{ex}}(\tilde{Y}_t|\tilde{\rho}) = \text{Tr}[\hat{K}_{\text{ex}}(\tilde{Y}_t)\tilde{\rho}\hat{K}_{\text{ex}}^\dagger(\tilde{Y}_t)]$. The trace distance is then also averaged over possible states $\tilde{\rho}$ to make the average distance independent of any initial state. For convenience, we consider $\tilde{\rho} = |\psi\rangle\langle\psi|$ as a pure state of a single qubit, i.e., $|\psi\rangle = \cos(\theta/2)|0\rangle + e^{i\phi}\sin(\theta/2)|1\rangle$, and the integral is over the Harr-measure, $d\mu_H = d\phi\sin(\theta)d\theta/(4\pi)$.

A. Comparison for qubit z -measurement

We begin with the qubit z -measurement. In this case, the Lindblad operator is $\hat{c} = \sqrt{\gamma/2}\hat{\sigma}_z$, and the exact measurement operator is given by \hat{K}_H in Eq. (68). Here, there is only one record variable to compute the exact map, $\tilde{Y}_t = Y_t$. Therefore, we calculate the average over the coarse-grained measurement results with their exact probability distribution $\wp_{\text{ex}}(Y_t|\tilde{\rho}) = \text{Tr}[\hat{K}_H(Y_t)\tilde{\rho}\hat{K}_H^\dagger(Y_t)]$. Using the average trace distance in Eq. (84) and the exact PDF, we perform analytical calculations using *Mathematica* and obtain results for different measurement operators shown in Table II (left column). To simplify the analytical calculation, we had to Taylor-expand the integrand of Eq. (84) to the 4th order in γ . We chose γ instead of Δt as our expansion parameter to consistently track the expansion orders of the time-related variables.

From the results in Table II, we see that all the average trace distances are of order of $\Delta t^{3/2}$, even that for the higher-order map \hat{K}_W we introduced. However, they have different pre-factors and our proposed operator \hat{K}_W gives the smallest distance to the exact trajectories. The operators from Itô and Guevara-Wiseman approaches give states with the largest average distance from the exact state.

B. Comparison for qubit's fluorescence measurement

For the second example, the Lindblad operator is $\hat{c} = \sqrt{\gamma}\hat{\sigma}_-$, with γ representing the qubit's fluorescence (decay) rate. We use the nearly exact version of the measurement operator derived in Eqs. (79) and (81), where we need the two types of coarse-grained measurement results Y_t and Z_t . Therefore, the average over the measurement results in Eq. (84) now becomes the average over both Y_t and Z_t , where the probability weight is replaced by

$$\wp_{\text{ex}}(\tilde{Y}_t|\tilde{\rho}) = \text{Tr}[\hat{K}_F(Y_t, Z_t)\tilde{\rho}\hat{K}_F^\dagger(Y_t, Z_t)], \quad (85)$$

given $\tilde{Y}_t = \{Y_t, Z_t\}$ and using the Kraus operator defined in Eq. (81). The statistical independence of Y_t and Z_t allows us to integrate the two variables directly with $\wp_{\text{ex}}(\tilde{Y}_t|\tilde{\rho})$. We performed the analytical calculations similarly to the z -measurement case and the results are presented in Table II (right column).

Again, our proposed measurement operator \hat{K}_W outperforms other approaches, this time by a pre-factor 1/2. We also note that \hat{K}_I and \hat{K}_R give exactly the same result for this example because the two maps coincide when $\hat{c}^2 = \hat{\sigma}_-^2 = 0$.

VII. CONCLUSION

As measurement records from real experiments are usually obtained with finite time resolution (Δt), existing tools used in processing the records to get quantum trajectories can easily lead to numerical errors in resulting quantum states. In this work, we have presented a systematic approach to evaluate the accuracy of quantum trajectory and to analyze what should be a good (Kraus) map based on the hierarchy of conditions: (A) valid quantum trajectory, (B) Lindblad evolution, and (C) valid average quantum evolution. The last can be broken down into three conditions: (C1) complete positivity, (C2) convex-linearity, and (C3) trace preservation.

Conditions	\hat{K}_I	\hat{K}_R	\hat{K}_G	\hat{K}_W
(A) VQT (two examples)	$\mathcal{O}(\Delta t)$			
(B) Lindblad solution	$\mathcal{O}(\Delta t)$		$\mathcal{O}(\Delta t^2)$	
(C) VAQE (Method I & II)	$\mathcal{O}(\Delta t)$		$\mathcal{O}(\Delta t^2)$	

TABLE III. Summary of the order of accuracy in Δt for the three hierarchy conditions (A), (B), and (C) for the existing maps. Note that VQT stands for the valid quantum trajectory and VAQE stands for valid average quantum evolution.

We considered the accuracy of these conditions at the second order in Δt , i.e., one order higher than traditional treatments. We then reviewed existing maps from the literature, finding that all considered approaches failed to satisfy the Lindblad evolution (B) and two of them, $\hat{K}_I(Y_t)$ and $\hat{K}_R(Y_t)$, failed to generate the valid average quantum evolution (C), to second order in Δt .

We therefore introduced a technique to construct measurement operators from a unitary system-bath interaction in the interaction-frame expanded to fourth order in the bath operator. For a single Lindblad operator and $\hat{H} = 0$, we have constructed a higher-order map $\hat{K}_W(Y_t)$ that satisfies all the desired conditions (B) and (C), to second order in Δt . We also showed that the higher-order map outperforms other approaches, giving the smallest distance to the exact trajectories, which is the strongest condition (A), at least for the two qubit examples: the qubit z -measurement and the qubit fluorescence measurement. Analytical results are summarized in Table II.

We can also summarize the accuracy of the hierarchy conditions (A), (B), and (C), which can be computed analytically for all approaches we considered in Table III. From bottom to top rows, the condition (C) is satisfied to $\mathcal{O}(\Delta t^2)$ if one uses the Guevara-Wiseman map, $\hat{K}_G(Y_t)$, or our proposed map, $\hat{K}_W(Y_t)$, while the condition (B) is satisfied only for $\hat{K}_W(Y_t)$. For the strongest condition (based on the two qubit examples, see Table II), all approaches give the average trace distance to the exact quantum trajectories at the order of $\mathcal{O}(\Delta t^{3/2})$ and above, i.e., the accuracy is only to $\mathcal{O}(\Delta t)$. As mentioned in the previous paragraph that our proposed map outperforms all others with the smallest prefactors of the average trace distance. Notably, the systematic hierarchy of assessing the map is consistent with the one-way implication diagram.

Given our analysis, we believe that our proposed map $\hat{K}_W(Y_t)$ will be useful when a high-accuracy calculation of quantum evolution is needed and a time resolution of measurement records cannot be assumed infinitesimal. Our immediate future work is to implement the new map to measurement records from the experiment of fluorescence measurement of transmon qubits, Ref [61], where the calculation of high-accuracy quantum trajectories is needed in multi-parameter estimation using sequential Monte Carlo method [62, 63]. Moreover, we will also explore the generalization to multiple Lindblad channels and

non-zero system's Hamiltonian in the forthcoming companion paper [64]. A final aspect that can be explored is the possibility of including the integrated record Z_t , Eq. (78), in a Kraus map to enhance the accuracy of individual trajectory calculation.

VIII. ACKNOWLEDGEMENT

NW thanks S. Suwanna for support during the time he worked on this project at Mahidol University, Thailand. NW was also supported by the Development and Promotion of Science and Technology Talents Project Thailand (DPST). AC acknowledges the support of the Griffith University Postdoctoral Fellowship scheme and Australian Research Council Centre of Excellence Program CE170100012. This research has received funding support from the NSRF via the Program Management Unit for Human Resources and Institutional Development, Research and Innovation (Thailand) [grant number B39G670018].

Appendix A: Complete positivity for averaged SMEs

In this section, we show the violation of the complete positivity condition (C1) of the averaged SME. We start with an example of a two-qubit system initialized in a maximally entangled state, $\rho_{AB}(t) = \frac{1}{2}(|00\rangle + |11\rangle)(\langle 00| + \langle 11|)$, where the first space encodes a qubit subsystem A, and the second space encodes an ancillary state (subsystem B).

The first-order averaged SME can be expressed for the combined system as

$$\rho_{AB}(t + \Delta t) = \rho_{AB}(t) + \Delta t \mathcal{D}[\hat{c} \otimes \hat{1}_B], \quad (\text{A1})$$

where $\hat{1}_B$ is the identity operator in the ancillary state space and \hat{c} acts on the qubit subsystem A. One example that the complete positivity condition (C1) is violated is the non-Hermitian measurement of qubit fluorescence. The corresponding Lindblad operator is defined $\hat{c} = \sqrt{\gamma/2} \hat{\sigma}_-$, where $\hat{\sigma}_- = \frac{1}{2}(\hat{\sigma}_x - i\hat{\sigma}_y)$ acting as a lowering operator on the qubit. Substituting the superoperator \mathcal{D} to the joint state, we have

$$\rho_{AB}(t + \Delta t) = \frac{1}{2} \begin{pmatrix} 1 & 0 & 0 & 1 - \gamma\Delta t/2 \\ 0 & \gamma\Delta t & 0 & 0 \\ 0 & 0 & 0 & 0 \\ 1 - \gamma\Delta t/2 & 0 & 0 & 1 - \gamma\Delta t \end{pmatrix}. \quad (\text{A2})$$

The lowest eigenvalue of the matrix in Eq. (A2) is

$$\lambda = -\frac{1}{4}[\gamma\Delta t + \sqrt{2(2 - \gamma\Delta t(2 - \gamma\Delta t))} - 2] \approx -\frac{(\gamma\Delta t)^2}{4}.$$

The condition (C1) is clearly violated as the lowest eigenvalue is negative, with the size of Δt^2 .

Appendix B: Derivation of the Itô operator

We can construct the Itô measurement operator for a finite time increment Δt from the measurement operator of an infinitesimal record $\hat{M}(y_s)$ found in Eqs. (25) and (28),

$$\hat{M}_1(y_s) = \hat{1} - \frac{1}{2}\hat{c}^\dagger \hat{c} dt + \hat{c} y_s dt + \frac{1}{2}\hat{c}^2 (y_s^2 dt^2 - dt). \quad (\text{B1})$$

by combining the operators for all $m = \Delta t/dt$ infinitesimal records defined as $\{y_s : s \in \{t, t+dt, \dots, t+(m-1)dt\}\}$, keeping terms up to only $\mathcal{O}(dt^2)$. We first compute the product of the unnormalized operators and take the continuum limit to get

$$\begin{aligned} \hat{M}_I(Y_t) &= \lim_{m \rightarrow \infty} \hat{M}_1(y_{t+(m-1)dt}) \cdots \hat{M}_1(y_{t+dt}) \hat{M}_1(y_t) \\ &= \lim_{m \rightarrow \infty} \prod_{s=t}^{t+(m-1)dt} \left[\hat{1} - \frac{1}{2}\hat{c}^\dagger \hat{c} dt + \hat{c} y_s dt + \frac{1}{2}\hat{c}^2 (y_s^2 dt^2 - dt) \right], \\ &= \hat{1} - \frac{1}{2}(\hat{c}^\dagger \hat{c} + \hat{c}^2) \Delta t + \lim_{m \rightarrow \infty} \sum_{s=t}^{t+(m-1)dt} (\hat{c} y_s dt + \frac{1}{2}\hat{c}^2 y_s^2 dt^2). \end{aligned} \quad (\text{B2})$$

In the last line above, in the mean square limit, we can show that the infinite sum, $\mathcal{Y} \equiv \sum_s y_s^2 dt^2$, has a stochastic variance converging to zero,

$$\begin{aligned} \lim_{m \rightarrow \infty} \text{E}\{\mathcal{Y}^2\} - \text{E}\{\mathcal{Y}\}^2 &= \lim_{m \rightarrow \infty} dt^4 \sum_s \text{E}\{y_s^4\} - dt^4 \sum_s \text{E}\{y_s^2\}^2, \\ &= \lim_{m \rightarrow \infty} 4\mu^2 \frac{\Delta t^3}{m^2} + 2\frac{\Delta t^2}{m} = 0, \end{aligned} \quad (\text{B3})$$

where we have used $\text{E}\{y_s\} = \mu$ and $\text{E}\{y_s^2\} = \mu^2 + 1/dt$. This means that we can replace the infinite sum \mathcal{Y} with

$$\begin{aligned} \langle y_s | \hat{\beta}^0 | 0 \rangle &= \sqrt{\wp_{\text{ost}}(y_s)} \\ \langle y_s | \hat{\beta}^1 | 0 \rangle &= \langle y_s | \hat{c} d\hat{B}^\dagger | 0 \rangle = \sqrt{\wp_{\text{ost}}(y_s)} y_s \hat{c} dt \\ \langle y_s | \hat{\beta}^2 | 0 \rangle &= \langle y_s | \hat{c}^2 (d\hat{B}^\dagger)^2 - \hat{c}^\dagger \hat{c} d\hat{B} d\hat{B}^\dagger | 0 \rangle = \sqrt{\wp_{\text{ost}}(y_s)} [\hat{c}^2 (y_s^2 dt - 1) - \hat{c}^\dagger \hat{c}] dt \\ \langle y_s | \hat{\beta}^3 | 0 \rangle &= \langle y_s | \hat{c}^3 (d\hat{B}^\dagger)^3 - \hat{c}^\dagger \hat{c}^2 d\hat{B} (d\hat{B}^\dagger)^2 - \hat{c} \hat{c}^\dagger \hat{c} d\hat{B}^\dagger d\hat{B} d\hat{B}^\dagger | 0 \rangle = \sqrt{\wp_{\text{ost}}(y_s)} [\hat{c}^3 (y_s^3 dt - 3y_s) - 2y_s \hat{c}^\dagger \hat{c}^2 - y_s \hat{c} \hat{c}^\dagger \hat{c}] dt^2 \\ \langle y_s | \hat{\beta}^4 | 0 \rangle &= \langle y_s | \hat{c}^4 (d\hat{B}^\dagger)^4 - \hat{c}^\dagger \hat{c}^3 d\hat{B} (d\hat{B}^\dagger)^3 - \hat{c} \hat{c}^\dagger \hat{c}^2 d\hat{B}^\dagger d\hat{B} (d\hat{B}^\dagger)^2 - \hat{c}^2 \hat{c}^\dagger \hat{c} (d\hat{B}^\dagger)^2 d\hat{B} d\hat{B}^\dagger \\ &\quad + (\hat{c}^\dagger \hat{c})^2 (d\hat{B} d\hat{B}^\dagger)^2 + (\hat{c}^\dagger)^2 \hat{c}^2 d\hat{B}^2 (d\hat{B}^\dagger)^2 | 0 \rangle \\ &= \sqrt{\wp_{\text{ost}}(y_s)} [\hat{c}^4 (y_s^4 dt^2 - 6y_s^2 dt + 3) - (3\hat{c}^\dagger \hat{c}^3 + 2\hat{c} \hat{c}^\dagger \hat{c}^2 + \hat{c}^2 \hat{c}^\dagger \hat{c}) (y_s^2 dt - 1) + (\hat{c}^\dagger \hat{c})^2 + 2(\hat{c}^\dagger)^2 \hat{c}^2] dt^2, \end{aligned} \quad (\text{C2})$$

where we have omitted the terms consisting the rightmost operator $d\hat{B}_t$ as $d\hat{B}_t | 0 \rangle = 0$.

We obtain the unnormalized high-order measurement operator with infinitesimal records as

$$\hat{M}_2(y_s) = \hat{M}_1(y_s) + \left[\frac{1}{24}(\hat{c}^\dagger \hat{c})^2 + \frac{1}{12}(\hat{c}^\dagger)^2 \hat{c}^2 + \hat{M}_h(y_s) \right] dt^2, \quad (\text{C3})$$

its stochastic mean,

$$\lim_{m \rightarrow \infty} \text{E}\{\mathcal{Y}\} = \lim_{m \rightarrow \infty} \mu^2 \frac{\Delta t^2}{m} + \Delta t = \Delta t, \quad (\text{B4})$$

and we obtain the unnormalized measurement operator for a finite time Δt using the Itô approach as

$$\hat{M}_I(Y_t) = \hat{1} + \frac{1}{2}\hat{c}^\dagger \hat{c} \Delta t + \hat{c} Y_t \Delta t, \quad (\text{B5})$$

where we have defined a coarse-grained record

$$Y_t \equiv \frac{1}{\Delta t} \int_t^{t+\Delta t} ds y_s = \lim_{m \rightarrow \infty} \frac{1}{\Delta t} \sum_{s=t}^{t+(m-1)dt} y_s dt. \quad (\text{B6})$$

We can also find a normalized factor for this operator by convolution, from a product of $\wp_{\text{ost}}(y_s)$ for y_s satisfying Eq. (29). Because they are all Gaussian functions, we find that a normalized factor is $\sqrt{\wp_{\text{ost}}(Y_t)}$, with a new ostensible probability

$$\wp_{\text{ost}}(Y_t) = \left(\frac{\Delta t}{2\pi} \right)^{1/2} \exp(-Y_t^2 \Delta t / 2). \quad (\text{B7})$$

Appendix C: Derivation of the high-order measurement operator

In this section we will show the detailed derivation of the high-order completely positive map from Eq. (58) which are the high-order expansion of the unitary $\hat{U}_{t+dt,t}$. Let us consider the coupling unitary operator in Eq. (21) and define

$$\hat{U}_{t+dt,t} = \exp(\hat{\beta}) = \sum_{k=0}^{\infty} \frac{\hat{\beta}^k}{k!}, \quad (\text{C1})$$

where $\hat{\beta} \equiv \hat{c} d\hat{B}^\dagger - \hat{c}^\dagger d\hat{B}$. The Taylor-expanded $\hat{\beta}$ up to 4th order (or equivalently to $\mathcal{O}[|d\hat{B}|^4]$) and compute matrix elements of $\langle y_s | \hat{U}_{t+dt,t} | 0 \rangle$ as

where $\hat{M}_1(y_s)$ is defined in Eq. (B1) and $\hat{M}_h(y_s)$ is accounted terms of the third and fourth order of expansion, defined as

$$\hat{M}_h(y_s) \equiv \frac{1}{6} [\hat{c}^3 (y_s^3 dt - 3y_s) - 2y_s \hat{c}^\dagger \hat{c}^2 - y_s \hat{c} \hat{c}^\dagger \hat{c}] + \frac{1}{24} [\hat{c}^4 (y_s^4 dt^2 - 6y_s^2 dt + 3) - (3\hat{c}^\dagger \hat{c}^3 + 2\hat{c} \hat{c}^\dagger \hat{c}^2 + \hat{c}^2 \hat{c}^\dagger \hat{c}) (y_s^2 dt - 1)]. \quad (\text{C4})$$

By computing the product of $\hat{M}_2(y_s)$ similarly to Appendix B and introducing a dummy index j for the infinitesimal record where $s = t + (j-1)dt$, we can construct the high-order measurement operator as

$$\hat{M}_W(Y_t) = \lim_{m \rightarrow \infty} \hat{M}_2(y_{t+(m-1)dt}) \cdots \hat{M}_2(y_{t+dt}) \hat{M}_2(y_t) \quad (\text{C5})$$

$$= \lim_{m \rightarrow \infty} \prod_{j=1}^m \left\{ \hat{M}_1(y_j) + \left[\frac{1}{24} (\hat{c}^\dagger \hat{c})^2 + \frac{1}{12} (\hat{c}^\dagger)^2 \hat{c}^2 + \hat{M}_h(y_j) \right] dt^2 \right\}, \quad (\text{C6})$$

$$= \hat{1} + \lim_{m \rightarrow \infty} \left\{ -\frac{1}{2} \binom{m}{m-1} \hat{c}^\dagger \hat{c} dt + \hat{c} \sum_j y_j dt + \frac{1}{2} \hat{c}^2 \left[\sum_j y_j^2 dt^2 - dt \binom{m}{m-1} + \sum_{j \neq j'} y_j y_{j'} dt^2 \right] + \frac{1}{4} \binom{m}{m-2} (\hat{c}^\dagger \hat{c})^2 dt^2 \right. \\ \left. - \frac{1}{2} dt \sum_j \binom{m-j}{1} y_j dt [\hat{c} \hat{c}^\dagger \hat{c} + \hat{c}^\dagger \hat{c}^2] + \frac{1}{4} \hat{c}^3 \left[\sum_j dt y_j \left(\sum_{j'} y_{j'}^2 dt^2 - dt \binom{m}{m-1} \right) \right] + \frac{1}{24} \binom{m}{m-1} (\hat{c}^\dagger \hat{c})^2 dt^2 \right. \\ \left. + \frac{1}{12} \binom{m}{m-1} (\hat{c}^\dagger)^2 \hat{c}^2 dt^2 + \sum_j \hat{M}_2(y_j) dt^2 \right\}, \quad (\text{C7})$$

$$= \hat{1} - \frac{1}{2} \hat{c}^\dagger \hat{c} \Delta t + \hat{c} \Delta t Y_t + \frac{1}{2} \hat{c}^2 [Y_t^2 \Delta t^2 - \Delta t] + \frac{1}{8} (\hat{c}^\dagger \hat{c})^2 \Delta t^2 - \frac{1}{4} (\hat{c} \hat{c}^\dagger \hat{c} + \hat{c}^\dagger \hat{c}^2) \Delta t^2 Y_t, \quad (\text{C8})$$

where we have used the coarse-grained record, Y_t , as used in Eq. (B6). The summation in the coefficient of $\hat{c} \hat{c}^\dagger \hat{c} + \hat{c}^\dagger \hat{c}^2$ in Eq. (C7) can be evaluated as

$$\lim_{m \rightarrow \infty} dt \sum_{j=1}^m (m-j) y_j dt = \int_t^{t+\Delta t} [\Delta t - (s-t)] y_s ds \equiv R_t. \quad (\text{C9})$$

We find that the integral $R_t = \frac{1}{2} \Delta t^2 Y_t - Z_t$, where Z_t is defined in Eq. (78). This then leads to $-\frac{1}{2} [\hat{c} \hat{c}^\dagger \hat{c} + \hat{c}^\dagger \hat{c}^2] (\frac{1}{2} \Delta t^2 Y_t - Z_t)$. Since we consider the second order in Δt and we know that $E\{Z_t^2\} = \mathcal{O}(\Delta t^3)$, we therefore only keep the lower-order coarse-grained record, Y_t , as appeared in the last term in Eq. (C8). Including Z_t in the map might improve the accuracy of individual quantum trajectories, which will be investigated in future work.

The other vanishing terms are a result of: (1) the property in Eq. (B4), which allows us to replace $\sum_j y_j^2 dt^2 - \Delta t = 0$; and (2) the terms converge to zero as $m \rightarrow \infty$.

Appendix D: Multi-variable integration

To compute the moments, the record variables are discretized into $m = \Delta t/dt$ segments. Again, introducing the index $s = t + (j-1)dt$, we have

$$E\{X_t^p\} = \lim_{m \rightarrow \infty} \left(\prod_{j=1}^m \int dy_j \wp_{\text{ost}}(y_j) \right) \left(\sum_{j=1}^m y_j dt e^{-\gamma j dt/2} \right)^p, \quad (\text{D1a})$$

$$E\{Y_t^p Z_t^q\} = \lim_{m \rightarrow \infty} \left(\prod_{j=1}^m \int dy_j \wp_{\text{ost}}(y_j) \right) \left(\frac{1}{\Delta t} \sum_{j=1}^m y_j dt \right)^p \left(\sum_{j=1}^m y_j dt [j dt - (t + \frac{\Delta t}{2})] \right)^q, \quad (\text{D1b})$$

where $p, q \in \{0, 1, 2\}$. Following $\wp_{\text{ost}}(y_j)$ in Eq. (27), it is straightforward to evaluate the mean via

$$\left(\prod_j \int dy_j \wp_{\text{ost}}(y_j) \right) \sum_j y_j = 0. \quad (\text{D2})$$

For the first moment of each variable in Eqs. (D1), the

three variables therefore have zero mean, i.e., $E\{X_t\} = E\{Y_t\} = E\{Z_t\} = 0$.

Similarly, one can compute to the second moment via

$$\left(\prod_j \int dy_j \wp_{\text{ost}}(y_j) \right) \sum_{j,j'} y_j y_{j'} = \sum_{j,j'} \frac{\delta_{j,j'}}{dt}. \quad (\text{D3})$$

Using the property in Eq. (D3), the resulting second moments are evaluated to the following integrals:

$$\begin{aligned} E\{X_t^2\} &= \int_t^{t+\Delta t} e^{-\gamma s} ds = \frac{2}{\gamma} e^{-\gamma(t+\Delta t/2)} \sinh(\gamma\Delta t/2), \\ E\{Y_t^2\} &= \frac{1}{\Delta t^2} \int_t^{t+\Delta t} ds = \frac{1}{\Delta t}, \\ E\{Z_t^2\} &= \int_t^{t+\Delta t} [s - (t + \Delta t/2)]^2 ds = \Delta t^3/12, \text{ and} \\ E\{Y_t Z_t\} &= \frac{1}{\Delta t} \int_t^{t+\Delta t} [s - (t + \Delta t/2)] ds = 0. \end{aligned} \quad (\text{D4})$$

Appendix E: Bayesian fluorescence map

Application of the Bayesian probability for the qubit fluorescence has been investigated in [57]. By considering a composite system (the two-level system and the photon) and assuming its initial state is a product state given by

$$|\psi_0\rangle = (a|e\rangle + b|g\rangle)|0\rangle, \quad (\text{E1})$$

where the qubit's initial state is a superposition state $a|e\rangle + b|g\rangle$, with $|a|^2 + |b|^2 = 1$, and the bath's initial state is assumed to be a vacuum state. The qubit's decay can be treated phenomenologically, by considering the probability of the transition (excited state to ground state) for a time length Δt . The probability of transition, emitting a single photon to the bath, given that the initial state of the qubit is $|e\rangle$ is $\wp(1|e) = \gamma\Delta t$, where γ is the qubit's decay rate. This gives the probability of no decay as $\wp(0|e) = 1 - \gamma\Delta t$. The qubit's state then evolves from

Eq. (E1) for the duration of time Δt to a final state given by

$$\begin{aligned} |\psi_f\rangle &= a\sqrt{\wp(0|e)}|e\rangle|0\rangle + a\sqrt{\wp(1|e)}|g\rangle|1\rangle + b|g\rangle|0\rangle \\ &= a\sqrt{1 - \gamma\Delta t}|e\rangle|0\rangle + a\sqrt{\gamma\Delta t}|g\rangle|1\rangle + b|g\rangle|0\rangle. \end{aligned} \quad (\text{E2})$$

From this initial and final state, we can construct the unitary operator for the composite system $\hat{U}_{t+\Delta t, t}$ and derive the Kraus operator via $|\psi_f\rangle = \hat{K}_{\text{F, Bay}}|\psi_i\rangle$.

Following Eq. (3), the bath's initial state is the vacuum state, i.e., $|e_0\rangle = |0\rangle$. The bath's final state will depend on the type of measurement considered. In this work, we consider the diffusive-type measurement, such as the homodyne detection. For consistency of the notation to our work and projecting to the homodyne eigenstate, the measurement operator derived in Ref. [57, 58] is given by

$$\hat{K}_{\text{F, Bay}}(Y_t) = \left(\frac{\Delta t}{2\pi}\right)^{\frac{1}{4}} e^{-Y_t^2 \Delta t/4} \begin{pmatrix} \sqrt{1 - \gamma\Delta t} & 0 \\ \sqrt{\gamma} Y_t \Delta t & 1 \end{pmatrix}. \quad (\text{E3})$$

The top-right element is simply the first order expansion of the exponential function of the top-right element in Eq. (73), while the bottom-right element corresponds to the zeroth-order of expansion of X_t defined in Eq. (74).

The quantum Bayesian approaches are trace preserving (C3), which can be shown as

$$\int dY_t \hat{K}_{\text{F, Bay}}^\dagger(Y_t) \hat{K}_{\text{F, Bay}}(Y_t) = \hat{1}. \quad (\text{E4})$$

However, the map gives the average trajectory agreeing with the (B) Lindblad master equation only to the first order in Δt . To see this, we expand $\hat{K}_{\text{F, Bay}}(Y_t)$ to second order in Δt . We find that it exactly coincides with $\hat{K}_{\text{G}}(Y_t)$ as defined in Eqs. (49) and (50) with $\hat{c} = \sqrt{\gamma}\hat{\sigma}_-$.

-
- [1] E. B. Davies, *Quantum Theory of Open Systems* (Academic Press, London, 1976).
 - [2] H. Breuer and F. Petruccione, *The Theory of Open Quantum Systems* (Oxford University Press, New York, 2002).
 - [3] M. A. Nielsen and I. L. Chuang, *Quantum Computation and Quantum Information: 10th Anniversary Edition* (Cambridge University Press, 2010).
 - [4] H. J. Carmichael, *An Open Systems Approach to Quantum Optics* (Springer, Berlin, 1993).
 - [5] H. M. Wiseman and G. J. Milburn, *Quantum Measurement and Control* (Cambridge University Press, 2009).
 - [6] N. Van Kampen, ed., *Stochastic Processes in Physics and Chemistry (Third Edition)* (Elsevier, Amsterdam, 2007).
 - [7] G. Lindblad, *Communications in Mathematical Physics* **48**, 119 (1976).
 - [8] L. Li, M. J. Hall, and H. M. Wiseman, *Physics Reports* **759**, 1 (2018), concepts of quantum non-Markovianity: A hierarchy.
 - [9] V. P. Belavkin, *Rep. Math. Phys.* **43**, A405 (1999).
 - [10] K. Jacobs, *Stochastic Processes for Physicists: Understanding Noisy Systems* (Cambridge University Press, 2010).
 - [11] E. B. Davies, *Communications in Mathematical Physics* **15**, 277 (1969).
 - [12] C. W. Gardiner, *Handbook of Stochastic Methods: For Physics, Chemistry and the Natural Science* (Springer-Verlag, Berlin, 1985).
 - [13] V. Belavkin, *Lecture Notes in Control and Information Sciences* (Springer, Berlin, 1988).
 - [14] V. P. Belavkin, *Journal of Multivariate Analysis* **42**, 171 (1992).
 - [15] A. Barchielli, *International Journal of Theoretical Physics* **32**, 2221 (1993).
 - [16] A. Barchielli, *Quantum Optics: Journal of the European Optical Society Part B* **2**, 423 (1990).
 - [17] H. M. Wiseman and G. J. Milburn, *Phys. Rev. A* **47**, 642 (1993).
 - [18] H. M. Wiseman and G. J. Milburn, *Phys. Rev. A* **47**, 1652 (1993).
 - [19] M. B. Plenio and P. L. Knight, *Rev. Mod. Phys.* **70**, 101 (1998).
 - [20] A. N. Korotkov, *Phys. Rev. B* **60**, 5737 (1999).

- [21] A. N. Korotkov, Phys. Rev. B **63**, 115403 (2001).
- [22] L. Diósi, Physics Letters A **129**, 419 (1988).
- [23] K. Jacobs and D. A. Steck, Contemporary Physics **47**, 279 (2006), <https://doi.org/10.1080/00107510601101934>.
- [24] J. Gambetta, A. Blais, M. Boissonneault, A. A. Houck, D. I. Schuster, and S. M. Girvin, Phys. Rev. A **77**, 012112 (2008).
- [25] N. Roch, M. E. Schwartz, F. Motzoi, C. Macklin, R. Vijay, A. W. Eddins, A. N. Korotkov, K. B. Whaley, M. Sarovar, and I. Siddiqi, Phys. Rev. Lett. **112**, 170501 (2014).
- [26] B. Q. Baragiola and J. Combes, Phys. Rev. A **96**, 023819 (2017).
- [27] D. A. Ivanov, T. Y. Ivanova, S. F. Caballero-Benitez, and I. B. Mekhov, Phys. Rev. Lett. **124**, 010603 (2020).
- [28] P. Guilmin, P. Rouchon, and A. Tilloy, arXiv:2212.00176 [quant-ph] (2022).
- [29] J. Steinmetz, D. Das, I. Siddiqi, and A. N. Jordan, Phys. Rev. A **105**, 052229 (2022).
- [30] H. Amini, M. Mirrahimi, and P. Rouchon, in *2011 50th IEEE Conference on Decision and Control and European Control Conference* (2011) pp. 6242–6247.
- [31] J. F. Ralph, K. Jacobs, and C. D. Hill, Phys. Rev. A **84**, 052119 (2011).
- [32] H. Amini, C. Pellegrini, and P. Rouchon, Russian Journal of Mathematical Physics **21**, 297 (2014).
- [33] P. Rouchon and J. F. Ralph, Phys. Rev. A **91**, 012118 (2015).
- [34] R. Vijay, C. Macklin, D. H. Slichter, S. J. Weber, K. W. Murch, R. Naik, A. N. Korotkov, and I. Siddiqi, Nature **490**, 77 (2012).
- [35] K. W. Murch, S. J. Weber, C. Macklin, and I. Siddiqi, Nature **502**, 211 (2013).
- [36] S. J. Weber, A. Chantasri, J. Dressel, A. N. Jordan, K. W. Murch, and I. Siddiqi, Nature **511**, 570 (2014).
- [37] A. Chantasri, M. E. Kimchi-Schwartz, N. Roch, I. Siddiqi, and A. N. Jordan, Phys. Rev. X **6**, 041052 (2016).
- [38] S. Hacoen-Gourgy, L. S. Martin, E. Flurin, V. V. Ramasesh, K. B. Whaley, and I. Siddiqi, Nature **538**, 491 (2016).
- [39] P. Campagne-Ibarcq, P. Six, L. Bretheau, A. Sarlette, M. Mirrahimi, P. Rouchon, and B. Huard, Phys. Rev. X **6**, 011002 (2016).
- [40] P. Six, P. Campagne-Ibarcq, I. Dotsenko, A. Sarlette, B. Huard, and P. Rouchon, Phys. Rev. A **93**, 012109 (2016).
- [41] P. Rouchon, Annual Reviews in Control **54**, 252 (2022).
- [42] G. Milstein, *Numerical Integration of Stochastic Differential Equations* (Springer, 1995).
- [43] I. Guevara and H. M. Wiseman, Phys. Rev. A **102**, 052217 (2020).
- [44] P. Goetsch and R. Graham, Phys. Rev. A **50**, 5242 (1994).
- [45] K. Jacobs and P. L. Knight, Phys. Rev. A **57**, 2301 (1998).
- [46] S. Gammelmark, B. Julsgaard, and K. Mølmer, Phys. Rev. Lett. **111**, 160401 (2013).
- [47] Y. Aharonov and L. Vaidman, in *Time in Quantum Mechanics*, edited by J. G. Muga, R. S. Mayato, and E. I. L. (Springer-Verlag Berlin Heidelberg, 2002) pp. 369–412.
- [48] I. Guevara and H. Wiseman, Phys. Rev. Lett. **115**, 180407 (2015).
- [49] A. Chantasri, I. Guevara, and H. M. Wiseman, New Journal of Physics **21**, 083039 (2019).
- [50] J. Steinbach, B. M. Garraway, and P. L. Knight, Phys. Rev. A **51**, 3302 (1995).
- [51] J. Gambetta and H. M. Wiseman, Journal of Optics B: Quantum and Semiclassical Optics **7**, S250 (2005).
- [52] A. Chantasri, I. Guevara, K. T. Laverick, and H. M. Wiseman, Physics Reports **930**, 1 (2021), unifying theory of quantum state estimation using past and future information.
- [53] H. M. Wiseman, Phys. Rev. A **56**, 2068 (1997).
- [54] H. M. Wiseman, “Squeezing and feedback,” in *Quantum Squeezing*, edited by P. D. Drummond and Z. Ficek (Springer Berlin Heidelberg, Berlin, Heidelberg, 2004) pp. 171–223.
- [55] C. W. Gardiner, A. S. Parkins, and P. Zoller, Phys. Rev. A **46**, 4363 (1992).
- [56] A. Chantasri, I. Guevara, and H. M. Wiseman, New Journal of Physics **21**, 083039 (2019).
- [57] A. N. Jordan, A. Chantasri, P. Rouchon, and B. Huard, Quantum Studies: Mathematics and Foundations **3**, 237 (2016).
- [58] P. Lewalle, S. K. Manikandan, C. Elouard, and A. N. Jordan, Contemporary Physics **61**, 26 (2020), <https://doi.org/10.1080/00107514.2020.1747201>.
- [59] A. N. Korotkov, Phys. Rev. A **65**, 052304 (2002).
- [60] R. Ruskov and A. N. Korotkov, Phys. Rev. B **67**, 241305 (2003).
- [61] M. Naghiloo, N. Foroozani, D. Tan, A. Jadbabaie, and K. W. Murch, Nature Communications **7**, 11527 (2016).
- [62] J. F. Ralph, S. Maskell, and K. Jacobs, Phys. Rev. A **96**, 052306 (2017).
- [63] C. Manoworakul, N. Wonglakhon, J. Ralph, H. M. Wiseman, and A. Chantasri, (In preparation).
- [64] N. Wonglakhon, H. M. Wiseman, and A. Chantasri, (In preparation).